

Response to Reviewer #1

We thank the reviewer for reviewing our manuscript and for providing detailed comments. The reviewer raised in particular several major concerns regarding the methodology employed in our study, which we address in detail below. As can be seen from our response, we feel that these issues can be resolved by better clarifying our methodology in the revised version of our manuscript.

Our responses are marked in bold font in the text below, in between the reviewer's comments.

Summary of the manuscript:

Authors have studied magnetosheath dawn-dusk asymmetries of the magnetic field (B), proton number density (n) and plasma flow speed(V) in the 2-D global Vlasiator simulation and compared the results with statistics from the THEMIS observations. The main conclusion made by the authors is that while the polarity of the asymmetries agrees with the THEMIS results, the magnitudes are in disagreement because Vlasiator is run with one set of conditions, whereas spacecraft observations show cumulation of the observations from different solar wind conditions and IMF orientations.

Overall evaluation of the manuscript:

Unfortunately, in its present form I am unable to recommend this manuscript for publication in the scientific literature for the following reasons:

1) There are no original ideas or new scientifically valid results. There have been several past studies of the magnetosheath properties using both spacecraft data and different plasma approximation (e.g., MHD, hybrid, kinetic-simulations). Some of these have been cited but not all: The bow shock is not the only source for magnetosheath plasma. Also magnetopause processes are important that can transport magnetospheric particles into the magnetosheath. The study of the dawn-dusk asymmetries of B, n and V using spacecraft data has already been done. If the motivation is to solely test the code robustness, by using the study of dawn-dusk asymmetries as a validation effort against spacecraft data, a technical paper may be more suitable.

We agree that there has been a number of observational studies of the dawn-dusk asymmetries of the parameters we selected for our study, as well as a few numerical studies using MHD models. However, we politely disagree with the reviewer regarding the lack of new results in our study.

In this manuscript, we present the first study of these asymmetries using a global hybrid-Vlasov model, which provides us with new information regarding those asymmetries. To our knowledge, this is the first in-depth quantification of these asymmetries using a hybrid-kinetic model. Part of our manuscript is indeed dedicated to validating our simulation results based on the comparison with previous works, but we also present novel results:

(1) We show that foreshock kinetic processes have a strong impact on the magnetosheath density, thus providing an answer to the long-standing question of the variability of this asymmetry, and reconciling the vastly different results obtained in previous studies [Paularena et al., 2001; Walsh et al., 2012; Dimmock et al., 2016]

(2) We investigate the influence of the IMF cone angle on the asymmetries, which has not been studied before, neither with spacecraft measurements nor with models, and show that the magnetic field asymmetry and the variability of the magnetosheath density increase when the cone angle is reduced from 45° to 30°.

(3) We investigate the influence of the Alfvén Mach number on the asymmetries, in a range of Mach numbers that is not easily accessible with observations, and show that the variability of the magnetosheath density and velocity is reduced at low Alfvén Mach numbers.

In the revised manuscript, we have reformulated part of the abstract (lines 12-13 and 17-21) and of the conclusions (lines 508-510) to better highlight these novel results.

Regarding the importance of magnetopause processes, we agree with the reviewer that they can indeed affect magnetosheath properties near the magnetopause.

In the revised manuscript, we added a brief mention to magnetopause processes (lines 40-43).

2) For scientific paper “more in depth” analysis of the physical mechanisms is required to address what differences are due to numerical issues, what are due to kinetic physics, and what are the mechanisms. For example, how are the magnetosheath densities > 4 explained, if solar wind density is 1? How are these results affected by grid-resolution.

According to MHD theory, the compression at the bow shock should indeed result in the magnetosheath density just downstream of the shock being at most four times larger than the solar wind density. This is what is observed downstream of the quasi-perpendicular portion of the bow shock in our numerical simulations (see the upper half of the top three panels in Fig. 6), where MHD theory mostly holds. At the quasi-parallel shock, on the other hand, kinetic processes become most prominent, and larger densities can be observed in the magnetosheath.

These large densities come essentially from density fluctuations in the foreshock, resulting in upstream densities that are already well above the plasma density in the pristine solar wind [see, for example, the numerical simulations presented in Omidi et al., 2014 and Turc et al., 2018; and the spacecraft measurements presented in the review by Eastwood et al., 2005]. When these patches of high density cross the bow shock, their fourfold compression results in downstream densities that exceed four times the solar wind density.

Such large densities in the magnetosheath, above the MHD limit, are a common feature in hybrid-kinetic simulations of the bow shock/magnetosheath system [see for example Figs. 9 and 10 in Omidi et al., 2014; Fig. 7 in Karimabadi et al., 2014]. We have added a few sentences in Section 3.3 of the manuscript (lines 343-346) to compare the magnetosheath density in our simulations with that in these previous numerical works.

Regarding the possible effects of grid resolution, the scale of these high density patches in the magnetosheath is much larger than the cell size, and thus they shouldn't be affected by the finite resolution in our simulations. Grid resolution, on the other hand, can impact which wave modes develop in the simulation [see Dubart et al., 2020, pre-print available in *Annales Geophysicae Discussions*: <https://www.ann-geophys-discuss.net/angeo-2020-24/>]. Previous works have shown that the compressional foreshock waves, the so-called 30 s waves, which are responsible for large-scale density fluctuations in the foreshock, are properly resolved in Vlasiator and their properties match those obtained from spacecraft measurements [Palmroth et al., 2015; Turc et al., 2018, 2019]. Also, foreshock transients such as cavitons and spontaneous hot flow anomalies, which can also result in density variations, develop as expected in the simulation [Blanco-Cano et al., 2018]. Therefore, the spatial resolution of our simulation is not expected to affect the plasma compression at the bow shock.

More discussion regarding the resolution is given below, as a response to another of the referee's comments. We have also added some discussion regarding the grid resolution in the revised manuscript (lines 444-454).

3) The Methodology of the present paper is flawed so no accurate scientific conclusions can be made at this time. The authors' conclusion, that the disagreement with the data and simulation is due to the fact that simulation is run for one set of conditions, whereas spacecraft data contains the history of IMF and solar wind, is only one possible reason. Paper fails to discuss the other, more plausible and likely more significant reasons listed below:

i) Code is run with 750 km/s solar wind speed. This condition occurs rarely as the average solar wind speed is slightly less than 400 km/s. Therefore, it is not logical or scientifically justified to compare the runs with 750 km/s solar wind velocity with the spacecraft statistics collected in the magnetosheath, when the solar wind flow preceding the THEMIS data collection is about 400 km/s. With higher solar wind speeds, the shock compression becomes stronger and one would expect higher magnetic field strengths downstream of the quasi-perpendicular shock than for solar wind speeds of 400 km/s.

While we agree with the reviewer that such fast speeds are rarely encountered in the solar wind at Earth, we will demonstrate that running the model with a 750 km/s solar wind speed is not an issue for the present study, and that our methodology is valid.

Firstly, the key parameter controlling the shock compression is the shock Mach number [e.g., Treumann et al., 2009], which indeed depends on the solar wind velocity, but also on other parameters such as the density, temperature and magnetic field strength, in the case of the magnetosonic Mach number. In our simulation, the upstream parameters are chosen such that the resulting Alfvén and magnetosonic Mach numbers have typical values for the solar wind at Earth: in our Runs 1 and 2A, the Alfvén Mach number M_A is 6.9 and the magnetosonic Mach number M_{ms} is 5.5, and our low Mach number run has $M_A = 3.4$ and $M_{ms} = 3.3$. Typical values for these Mach numbers at Earth are $2.5 < M_A < 12$ and $2 < M_{ms} < 7$ [Winterhalter & Kivelson, 1988]. Therefore, despite the large solar wind speed, we have a typical compression ratio at the bow shock with our input parameters (see Fig. 5). We will add a sentence in Section 2.2, where the simulation runs are described, to indicate that the Mach number values in our runs are typical values at Earth.

Second, we would like to point out that all observational studies of magnetosheath asymmetries rely on the assumption that the variation of the shock compression is relatively small in the range of solar wind conditions encountered at Earth, and thus that magnetosheath parameters can be normalised to their solar wind counterparts to obtain the average distribution of magnetosheath properties. This normalisation is essential to observational studies, which are based on compilations of spacecraft measurements in the magnetosheath associated with a wide variety of solar wind conditions. Global maps of normalised magnetosheath parameters are presented for example in Paularena et al. [2001], Longmore et al. [2005] and Dimmock et al. [2013-2017]. Walsh et al. [2012] present both raw and normalised magnetosheath parameters, and the latter are more narrowly-distributed around the results from MHD simulations. The only instance in which Dimmock et al. [2017] do not use a normalised parameter is for the ion temperature, because of cross-calibration issues when comparing temperature measurements from different spacecraft (THEMIS in the magnetosheath and ACE or Wind in the solar wind). Moreover, Dimmock et al. [2017] compare the levels of magnetosheath asymmetries for solar wind velocities below and above 400 km/s (splitting their data set into two halves), and find no significant change in the asymmetries between these two ranges of solar wind velocities.

Large solar wind speeds may strongly affect the flank magnetosheath parameters, as large solar wind speeds are conducive to the development of the Kelvin-Helmholtz instability (KHI) at the magnetopause [e.g. Kavosi & Raeder, 2015]. However, our study concentrates on magnetosheath asymmetries in the plane containing the IMF vector, while KHI develops in the plane that is perpendicular to the IMF (e.g. in the equatorial plane for a northward IMF). Therefore, our results would not be affected by the KHI.

Therefore, the large solar wind speeds in our simulations are not an issue to quantify the magnetosheath asymmetry levels away from the magnetopause, and the normalisation of the data to the solar wind quantities together with the typical shock Mach numbers and compression ratio in our simulations ensure that the comparison with spacecraft observations is relevant. In Section 2.3 of the revised manuscript, we now explain in more detail our approach and its validity.

ii) The runs use upstream solar wind density of $1/cc$, which would result in a maximum downstream density of about $4/cc$ downstream of quasi-perp shock. Assuming the values of $1-4/cc$, the ion inertial length would be 228 km to 114 km in the magnetosheath, respectively, and for higher densities these scales get even smaller. The paper does not describe what the coordinate-space resolution is used for the runs. In order to appropriately resolve the physical ion scales, the Vlasiator should use about 5 to 10 cells/ion inertial length, which requires coordinate space resolution at the minimum of about 20-40 km, otherwise the kinetic effects can artificially dominate at larger length scales than in the real system. Furthermore, if the ion inertial scale at the bow shock is not appropriately resolved, the results pertaining to kinetic shock physics are physically meaningless or exaggerated.

The resolution of our grid in ordinary space is 227 km, which corresponds to one ion inertial length in the solar wind. As shown by numerous works, this resolution is sufficient to capture most ion kinetic processes in a simulation, and yields results that are in good agreement with spacecraft observations. In this, we respectfully disagree with the reviewer's statement that one would require 5-10 cells per ion inertial length in hybrid kinetic simulations.

We kindly refer the reviewer to the works of Omidi and colleagues [e.g., Omidi et al., 2014, 2016] and Blanco-Cano and colleagues [e.g., Blanco-Cano et al., 2006, 2009], in which a cell size of 1 solar wind ion inertial length is also used, allowing detailed investigations of ion kinetic processes in the foreshock and the magnetosheath. In the simulations of Shi et al. [2013, 2017] the spatial resolution is 1 to 2 cells per ion inertial length, depending on the position in the simulation domain. Karimabadi et al. [2014] present the results of 7 runs, most of them with a resolution of 2 cells per ion inertial length. The run with the best resolution has 4 cells per ion inertial length, but at the expense of the size of the simulation domain.

The results of these models (Vlasiator included) pertaining to ion kinetic processes have been extensively validated against spacecraft measurements [e.g., Sibeck et al., 2008, Blanco-Cano et al., 2011, Palmroth et al., 2015, Turc et al., 2019]. They have predicted kinetic phenomena such as foreshock bubbles [Omidi et al., 2010] and cavitons [Blanco-Cano et al., 2009] that have been later on been confirmed in spacecraft measurements [Archer et al., 2015; Kajdic et al., 2011].

At the shock front, a cell size of 1 ion inertial length or larger may not correctly evaluate the gradient in the ramp. However, the hybrid-Vlasov formalism based on distribution functions enables the use of a slope limiter which allows for total variation diminishing evolution of discontinuities and steep slopes even at somewhat lower resolution. The shock transition is therefore well described in our simulations, and the downstream parameters are correctly modelled.

The study we present here focuses on the large-scale distribution of magnetosheath properties. Therefore, the spatial resolution of 1 cell per ion inertial length in our Vlasiator runs is sufficient to study global magnetosheath parameters and how they are impacted by ion kinetic physics. We have added a discussion on the spatial resolution in our simulations in the revised version of the manuscript (lines 444-454).

iii) Since the B , n and V are MHD quantities, authors should also run their case exactly with same parameters using the major global, state-of-the-art 3-D MHD codes available through Community Coordinated Modeling Center and compare their Vlasiator results with these.

Magnetosheath asymmetries have been already studied using MHD models in previous studies, as described in the Introduction [Walsh et al., 2012; Dimmock et al., 2013]. The results of Walsh et al. [2012] show in particular that the magnitude of the asymmetries is larger in their MHD simulations than in the observations. Their interpretation is similar as

ours: the asymmetries are larger in the simulations because they are run for a single IMF orientation, while the observations combine many different IMF orientations.

We have expanded the comparison to previous MHD simulations in the Discussion section of the revised manuscript (lines 467-469), but we do not feel that running new MHD simulations will bring novel information that is not already reported in the literature.

Recommendation:

While I cannot recommend this paper for publication at this time, I hope the authors will use this feedback as an opportunity to improve the paper, and for transparency include additional missing information (e.g., the grid-resolution etc.). This work requires significant further code validation efforts in a global scale, where the effects of spatial grid-resolution are systematically studied, so that the results can be correctly interpreted.

Please see the specific comments below that need to be addressed after which the paper may eventually become suitable for scientific literature:

We thank the reviewer for this very detailed set of suggestions on how to further proceed with this study. However, we believe that our methodology is appropriate for the present study, and that our conclusions are well supported by the analysis of our numerical results, as detailed in our responses to the reviewer's previous comments (see above).

Incidentally, we would like to mention that a typical Vlasiator run requires from a few to tens of million CPU hours. Performing a new set of runs as suggested by the reviewer is extremely costly, and thus cannot be done on a short notice, as it requires months of planning, application for computing resources, running and validation of the model's outputs.

Specific comments:

1. Calculate the statistical solar wind and IMF condition from THEMIS statistics used in the paper.
2. Plot and show a spatial map in x-y -plane for each run of the i) ion inertial length, ii) ion gyro-radius and iii) plasma beta, and collect a mean, minimum and maximum values of these at the central magnetosheath where the statistics pertaining to study is being collected during the course of the simulation.
3. Re-run Vlasiator with the statistical conditions and with the appropriate resolution (whichever length-scale is the smallest). For plasma beta of 1, the both length-scales should be the same. Compare the results with those in the present manuscript.
4. Add details and benchmarking how the phase space velocity distributions are processed to calculate n and V in 2-D-plane (as one can cut a 3-D velocity distribution in infinite ways). Show how the processing of the velocity distribution functions affects the results. Convince the reader of the validity of this processing at different regions in the magnetosheath.

While our simulation domain is 2D in ordinary space, the velocity space, in which the velocity distribution functions evolve, is 3D in Vlasiator. Therefore, no 2D cut is performed in the ion velocity distribution functions. The density and velocity are calculated as the zeroth and first velocity moments of the distribution functions, i.e., by integrating the distribution function over the velocity space, based on plasma kinetic theory. This approach is valid everywhere in the simulation domain. To clarify this, we have added a sentence in Section 2.1 explaining that the macroscopic plasma parameters are obtained by integrating the velocity distribution functions (lines 136-138).

5. Re-run Vlasiator with a) old-set of parameters shown in this manuscript while appropriately resolving these length-scales and compare with the results from original resolution.

6. Ion and electron temperatures are an important quantity to demonstrate the dawn-dusk asymmetry. It will be very interesting to see these two parameters, and the perpendicular and parallel temperatures.

Vlasiator is a hybrid model, which describes ion kinetic physics but treats electrons as a fluid. Therefore, it cannot be used to study electron temperatures in the magnetosheath. As concerns the ion temperature, we decided to leave it for future work, as we think its investigation warrants a paper of its own (as was done for example by Dimmock et al., 2015 for the ion temperature asymmetry in the magnetosheath as observed by the THEMIS spacecraft). Here, we chose to concentrate on the magnetic field strength, plasma density and bulk velocity, and how they vary as a function of the cone angle and the Alfvén Mach number.

7. Since the majority of the quantities compared in this study can also be obtained by the MHD global simulation, I suggest the authors also run the same solar input in the CCMC to compare with all the other three major MHD models and show the advantage of Vlasiator results.

As mentioned earlier, MHD simulations of magnetosheath asymmetries have already been performed by Walsh et al. [2012] and provide results consistent with our findings.

8. What is the “zebra stripes” structure on the dusk side, are those physical waves (which wave-mode) or a grid oscillation?

These are physical oscillations, which are well resolved in the simulation as their wavelength is significantly larger than the cell size. The properties of these oscillations are consistent with that of the overshoot of the quasi-perpendicular bow shock, which has been observed for example by the ISEE and the Cluster spacecraft [Livesey et al., 1982; Bale et al., 2005]:

**- their amplitude decays when moving further away from the shock front [Saxena et al., 2005].
- their wavelength is related to the ion gyroradius [Saxena et al., 2005]. This is evidenced by their smaller scale in Run 2B, where the IMF strength is doubled, and thus the gyroradius is smaller.**

- their amplitude is related to the upstream Mach number [Livesey et al., 1982]. It is much smaller in Run 2B (low M_A run), where the oscillations are barely visible in Figs 1, 3 and 6, than in the other two runs.

Investigating in more detail the properties of these oscillations and their relevance for magnetosheath transport processes is a study of its own, which is currently under way.

9. From MHD the maximum shock compression ratio would give magnetosheath densities of 4/cc if the density in the solar wind is 1/cc. Here the maximum density in the magnetosheath is 6/cc. Is this a kinetic effect and what is the physical mechanism to generate that? How is the area of the $> 4/cc$ density regions in the magnetosheath dependent on the ion gyro-radius/inertial scale and grid resolution when compared to MHD simulations that are run with the same parameters and same resolution?

As discussed above, these high density patches in the magnetosheath are most likely due to density enhancements in the foreshock which are further compressed upon crossing the bow shock. The density enhancements in the foreshock are due to compressional waves and transient structures. These phenomena are not described in MHD models, as the foreshock is inherently a kinetic structure. These results are therefore not comparable with MHD, where such phenomena do not exist.

The scale of these density enhancements is related to that of the foreshock ULF waves, which modulate the foreshock parameters, including the density [e.g., Blanco-Cano et al., 2006; Turc et al., 2018]. In previous studies, we have shown that the properties of these waves in our simulations are described at their correct scales and are in excellent agreement with spacecraft observations [Palmroth et al., 2015; Turc et al., 2018, 2019].

Minor comments:

1. The Discussion and Conclusions are repetitive. This could be made more concise.

We feel that the content of these two sections is appropriate and that they are complementary rather than repeating each other. As no concrete suggestions for shortening were given, we were not able to identify which parts the reviewer found redundant.

2. The referencing is inadequate. Authors should extend their citations to include some of the following. Please see previous global hybrid simulation studies of the magnetosheath (e.g. by Y. Lin et al. (2001-2020), H. Karimabadi et al., N. Omid et al.) and several missing studies related to spacecraft observations and statistics of the various foreshock transient that modify magnetosheath properties (e.g., F. Plaschke et al. (2013-2019), D. Turner et al., H. Hietala et al. (2009-2018), T. Liu et al. (2017-2019), H. Zhang et al. (2013-),) as well as leakage of magnetospheric particles into the magnetosheath by various processes (e.g., I. Cohen et al. 2017; K. Sorathia et al., 2019), and due to local magnetosheath physics (e.g., P. Gary et al., 2006 A. Retino et al. 2007, D. Sundkvist et al. 2007, J. Soucek et al. (2008-2015), V. Genot et al. (2001-2009), T. Phan et al., 2018).

We have added some of these references regarding magnetosheath properties in our introduction. We have also added a new paragraph in our introduction describing previous hybrid simulations, which include some of the references listed above (lines 111-118).

References (not previously included in the manuscript bibliography)

Archer, M. O., Turner, D. L., Eastwood, J. P., Schwartz, S. J., & Horbury, T. S.: Global impacts of a Foreshock Bubble: Magnetosheath, magnetopause and ground-based observations, *Planetary and Space Science*, 106, 56, doi:10.1016/j.pss.2014.11.026, 2015.

Bale, S. D., Balikhin, M. A., Horbury, T. S., Krasnoselskikh, V. V., Kucharek, H., Möbius, E., Walker, S. N., Balogh, A., Burgess, D., Lembège, B., Lucek, E. A., Scholer, M., Schwartz, S. J., & Thomsen, M. F.: Quasi-perpendicular Shock Structure and Processes, *Space Science Reviews*, 118, 161, doi:10.1007/s11214-005-3827-0, 2005.

Blanco-Cano, X., Omid, N., & Russell, C. T.: Macrostructure of collisionless bow shocks: 2. ULF waves in the foreshock and magnetosheath, *Journal of Geophysical Research (Space Physics)*, 111, A10205, doi:10.1029/2005JA011421, 2006.

Blanco-Cano, X., Omid, N., & Russell, C. T.: Global hybrid simulations: Foreshock waves and cavitons under radial interplanetary magnetic field geometry, *Journal of Geophysical Research (Space Physics)*, 114, A01216, doi:10.1029/2008JA013406, 2009.

Blanco-Cano, X., Kajdič, P., Omid, N., & Russell, C. T.: Foreshock cavitons for different interplanetary magnetic field geometries: Simulations and observations, *Journal of Geophysical Research (Space Physics)*, 116, A09101, doi:10.1029/2010JA016413, 2011.

Blanco-Cano, X., Battarbee, M., Turc, L., Dimmock, A. P., Kilpua, E. K. J., Hoilijoki, S., Ganse, U., Sibeck, D. G., Cassak, P. A., Fear, R. C., Jarvinen, R., Juusola, L., Pfau-Kempf, Y.,

Vainio, R., & Palmroth, M.: Cavitons and spontaneous hot flow anomalies in a hybrid-Vlasov global magnetospheric simulation, *Annales Geophysicae*, 36, 1081, doi:10.5194/angeo-36-1081-2018, 2018.

Dubart, M., Ganse, U., Osmane, A., Johlander, A., Battarbee, M., Grandin, M., Pfau-Kempf, Y., Turc, L., and Palmroth, M.: Resolution dependence of magnetosheath waves in global hybrid-Vlasov simulations, *Ann. Geophys. Discuss.*, <https://doi.org/10.5194/angeo-2020-24>, in review, 2020.

Eastwood, J. P., et al.: The Foreshock, *Space Science Reviews*, 118, 41, doi:10.1007/s11214-005-3824-3, 2005.

Kajdič, P., Blanco-Cano, X., Omid, N., & Russell, C. T.: Multi-spacecraft study of foreshock cavitons upstream of the quasi-parallel bow shock, *Planetary and Space Science*, 59, 705, doi:10.1016/j.pss.2011.02.005, 2011.

Karimabadi, H., Roytershteyn, V., Vu, H. X., Omelchenko, Y. A., Scudder, J., Daughton, W., Dimmock, A., Nykyri, K., Wan, M., Sibeck, D., Tatineni, M., Majumdar, A., Loring, B., & Geveci, B.: The link between shocks, turbulence, and magnetic reconnection in collisionless plasmas, *Physics of Plasmas*, 21, 062308, doi:10.1063/1.4882875, 2014.

Kavosi, S., & Raeder, J.: Ubiquity of Kelvin-Helmholtz waves at Earth's magnetopause, *Nature Communications*, 6, 7019, doi:10.1038/ncomms8019, 2015.

Livesey, W. A., Kennel, C. F., & Russell, C. T.: ISEE-1 and -2 observations of magnetic field strength overshoots in quasi-perpendicular bow shocks, *Geophysical Research Letters*, 9, 1037, doi:10.1029/GL009i009p01037, 1982.

Omid, N., Eastwood, J. P., & Sibeck, D. G.: Foreshock bubbles and their global magnetospheric impacts, *Journal of Geophysical Research (Space Physics)*, 115, A06204, doi:10.1029/2009JA014828, 2010.

Omid, N., Sibeck, D., Gutynska, O., & Trattner, K. J.: Magnetosheath filamentary structures formed by ion acceleration at the quasi-parallel bow shock, *Journal of Geophysical Research (Space Physics)*, 119, 2593, doi:10.1002/2013JA019587, 2014.

Omid, N., Berchem, J., Sibeck, D., & Zhang, H.: Impacts of spontaneous hot flow anomalies on the magnetosheath and magnetopause, *Journal of Geophysical Research (Space Physics)*, 121, 3155, doi:10.1002/2015JA022170, 2016.

Palmroth, M., et al.: ULF foreshock under radial IMF: THEMIS observations and global kinetic simulation Vlasator results compared, *Journal of Geophysical Research (Space Physics)*, 120, 8782, doi:10.1002/2015JA021526, 2015.

Saxena, R., Bale, S. D., & Horbury, T. S.: Wavelength and decay length of density overshoot structure in supercritical, collisionless bow shocks, *Physics of Plasmas*, 12, 052904, doi:10.1063/1.1900093, 2005.

Shi, F., Lin, Y., & Wang, X.: Global hybrid simulation of mode conversion at the dayside magnetopause, *Journal of Geophysical Research (Space Physics)*, 118, 6176, doi:10.1002/jgra.50587, 2013.

Shi, F., Cheng, L., Lin, Y., & Wang, X.: Foreshock wave interaction with the magnetopause: Signatures of mode conversion, *Journal of Geophysical Research (Space Physics)*, 122, 7057, doi:10.1002/2016JA023114, 2017.

Sibeck, D. G., Omidi, N., Dandouras, I., & Lucek, E.: On the edge of the foreshock: model-data comparisons, *Annales Geophysicae*, 26, 1539, doi:10.5194/angeo-26-1539-2008, 2008.

Turc, L., Roberts, O. W., Archer, M. O., Palmroth, M., Battarbee, M., Brito, T., Ganse, U., Grandin, M., Pfau-Kempf, Y., Escoubet, C. P., & Dandouras, I.: First Observations of the Disruption of the Earth's Foreshock Wave Field During Magnetic Clouds, *Geophysical Research Letters*, 46, 12,644, doi:10.1029/2019GL084437, 2019.

Winterhalter, D., & Kivelson, M. G.: Observations of the Earth's bow shock under high Mach number/high plasma beta solar wind conditions, *Geophysical Research Letters*, 15, 1161, doi:10.1029/GL015i010p01161, 1988.

Response to Reviewer #2

We thank the referee for their positive feedback on our manuscript and for their insightful remarks. Please find below our point-by-point response in bold font.

This manuscript describes 2D simulations of the dayside magnetosheath using the hybrid Vlasiator code, for three different upstream conditions (one in the noon-midnight plane, and two in the GSE equatorial plane). The authors appropriately describe the capabilities as well as the issues and shortcomings pertaining to this hybrid model. The detailed description of the challenges of magnetosheath studies using spacecraft observations is also highly appropriate. The explanations provided regarding the numerical results of magnetosheath asymmetries of parameters (B, density, and velocity) downstream of the Q_{para} and Q_{perp} bow shock regions as a function of angle from the Sun-Earth line are plausible, though perhaps not the only possible explanations. Comparing the numerical simulation results with magnetosheath observations by the THEMIS spacecraft is also highly appropriate.

There are two significant concerns with the manner in which the study results are presented. These ought to be fairly easily addressed, but are important because they directly affect most of the figures and results presented in this study:

1) Magnetosheath parameters determined from the numerical simulations within each spatial bin and for the time interval used are presented as averages; whereas the magnetosheath parameters determined from spacecraft observations are presented as medians. In order to ensure that the comparisons between simulations and observations are meaningful, the same statistical measure should be used for both (ideally medians, to avoid outlier kinetic effects due to processes at the bow shock convected into specific magnetosheath bins from unduly influencing the overall average value). An alternative is to demonstrate that within the magnetosheath bins, the distribution of values used to determine the spatial and temporal average is Gaussian, so that the average and median values are the same.

Thank you for pointing this out, we should indeed have used the same statistical measure to quantify the “global” value of the asymmetry in each run.

We would like to clarify that the magnetosheath parameters were computed using the same methodology both in the numerical simulations and the spacecraft observations, as averages inside each spatial bin. We chose to use averages so that our results are comparable to the statistical results presented in Dimmock et al. [2017]. We note however that Walsh et al. [2012] used median values inside the spatial bins rather than mean values.

In order to check that our results are not sensitive to using median or mean values, we calculated the asymmetries based on the median value in each bin. We found that both the mean and the median yield very similar asymmetry levels. This is now mentioned in the revised manuscript at lines 206-210.

After carefully trying out both median and mean values as indicators of the “global” asymmetry level, we came to the conclusion that the large variation of the asymmetry level from bin to bin in each simulation makes both of these problematic. To give a better description of our results, in the revised manuscript, we have given instead the range of values for each asymmetry. For example the magnetic field asymmetry in the central magnetosheath in Run 1 ranges between 0 and 15%, and compare it with the 5-10% values in Dimmock et al. [2017] (see lines 266-269).

2) It is difficult to judge the robustness of the results, because there are no estimates of the statistical spread (uncertainties) associated with the averages (or medians). From the simulations, sampling in appropriately sized sub-spatial and sub-temporal bins to provide e.g., standard deviations (or quartiles) used in the estimate of the asymmetry would instill considerable confidence that the percentage of asymmetry results are robust. Similarly for the THEMIS observations, it would be more appropriate if statistical estimates representing the range of values within each bin are determined and then used to estimate the range of values (measure of uncertainty) for the percentages of asymmetry for the various plasma parameters.

Thank you for this suggestion. In the revised manuscript, we have added error bars to the asymmetry plots (line plots in Figures 1, 3, 6 and 7). As done in Dimmock et al. [2017], we estimate the error on the magnetosheath parameters as the standard error of the mean (standard deviation divided by the square root of the size of the bin sample). We then use this error to calculate the minimum and maximum values of the asymmetry in each bin, which determines the extent of the error bars in the asymmetry plots. The estimation of the error is described at lines 210-212 and 226-228.

The error bars in our numerical results are much smaller than for the observational spacecraft data set, most likely because of the steady upstream conditions in our simulations.

Minor issues:

Line 268: considerable -> considerably

Figure 4: Should label which side of the plot corresponds to Q_{para} , and which side corresponds to Q_{perp} .

Line 341: magnetosheah -> magnetosheath

Thank you for picking up these typos, we have corrected them in the revised manuscript. We have added the suggested labels on Figure 4.

Response to Reviewer #3

We thank the reviewer for their careful examination of our manuscript and their constructive comments. Please find below our point-by-point response in bold font.

The paper describes the Earth magnetosheath response to the solar wind inflow using the Vlasiator code. The focus is put on the various asymmetries of plasma and magnetic parameters in three cases with varying IMF orientation and Alfvén Mach number. The results are then compared to an analysis of THEMIS observations which was published previously (Dimmock et al.'s papers). The objectives are sound, the code and the analysis appropriate, however a number of key points make the paper not mature enough in the present form. They are listed first, then minor issues follow.

Major points:

- References: the references to previous works are not adequate. Concerning hybrid codes for the magnetosheath, the literature was already vast before Vlasiator and 6D simulations of solar wind / planetary plasma interactions exist, e.g. Travnicek et al., 2007 (GRL), Hercik et al., 2013 (JGR), Modolo et al., 2017 (PSS), ... For magnetosheath asymmetries, see the works with Cluster data of Génot et al., and with ISEE data of Tatrallyay et al. For the discussions on Alfvén Mach number effects see Lavraud & Borovsky, 2008.

Thank you for providing these references, we have added them to the introduction in the revised manuscript (lines 68-70 and 111-118).

- Foreshock effects: it seems to me that the foreshock effects are over emphasized. Actually the perturbations linked to turbulence processes in the magnetosheath are more directly connected to effects associated to the physics of the parallel shock than to the foreshock itself which lies upstream of the shock. In that respect I disagree with the last sentence of the abstract and similar statements in the paper (for instance l353). Could the authors demonstrate why the foreshock is so important and for which effects it should be distinguished with the parallel shock?

We emphasized the importance of the foreshock because the density variations in the quasi-parallel magnetosheath largely come from density variations that are already present in the foreshock and that are amplified when crossing the bow shock (see also our response to the point 2 raised by Reviewer #1). Also, these alternating patches of higher and lower densities in the magnetosheath appear to be associated with irregularities of the shock front, whose scale is comparable to that of the foreshock waves. Previous studies have established that foreshock waves modulate the shape of the shock front [e.g., Burgess, 1995]. Finally, the lower density and velocity variability at lower Mach numbers may be related to the lower amplitude of the foreshock disturbances, or to their smaller scales.

We fully agree with the reviewer that the quasi-parallel shock physics likely also plays an important role in the quasi-parallel magnetosheath, and that bow shock and foreshock effects are hard to disentangle in this global context. In the revised manuscript, we have reworded the ending of the abstract (lines 18-19) and the relevant parts in the discussion and conclusions (lines 426-427, 496, 519, 524-525 and 533) to include quasi-parallel shock physics together with foreshock processes. We have also added more discussion as to how the foreshock affects the quasi-parallel magnetosheath, as detailed just above (lines 426-432).

- Kinetic effects: on l300 simulation results on density asymmetry are opposed to those coming from an analysis of MHD equations. The authors point to kinetic effects. Why is it that kinetic effects matter specifically on this issue and not on other where simulations and MHD match? This requires more discussion. Even though this may be outside the scope of the paper, a comparison

with 3D MHD simulation (for instance available at CCMC) would help pointing to specific kinetic effects inherent to the Vlasiator code.

We fully agree with the reviewer that it is rather surprising that one of our results regarding the plasma density asymmetry contradict MHD predictions, while a good agreement is found for all other parameters. We thought that this may stem from the fact that foreshock and quasi-parallel shock processes control to a great extent the spatial variations of the density in the quasi-parallel magnetosheath. Because the density asymmetry was more sensitive than the magnetic field strength or the plasma velocity to kinetic processes in the quasi-parallel flank, we argued that kinetic effects might dominate over fluid processes to explain the inconsistency.

However, after reconsidering our quantification of the “global” value of the asymmetries in the different runs, prompted by the first comment of Reviewer #2, we now find that the variation of the density asymmetry with the Mach number is actually inconclusive. Our statement regarding the decrease of the density asymmetry level at low Mach number, which contradicts MHD predictions, was based on the median values of the asymmetry level in the different runs, which were shown to change from -5% (Runs 1 and 2A) to -2% (Run 2B). However, the standard deviations associated with these median values are 5%, 4% and 2% for Runs 1, 2A and 2B, respectively. Also, when comparing visually the curves displayed in Figure 6d-e, there is no evident difference between the different runs, again due to the large variation from bin to bin.

We have therefore reformulated the paragraph at lines 358-366 to state that there is no conclusive difference in the density asymmetry level between the different runs. We thank the reviewer for drawing our attention to this point that helped us resolve the apparent contradiction between MHD and kinetic modelling results.

- Global approach: the model is 2D in space and the magnetopause is not completely resolved such that a model magnetopause needs to be used. This puts limitation on the term "global" to qualify the simulations. I wonder if the compression/expansion in this limited 2D space can be adequately compared with the real 3D situation. Could the authors discuss this aspect? or point to literature as this has surely been already addressed.

We apologize for the lack of clarity regarding the magnetopause description in our simulations. The magnetopause is self-consistently described in our simulation, and its position is determined by pressure balance, just like Earth’s magnetopause. A reliable method to evaluate the magnetopause position in numerical simulations is for example based on the magnetosheath flow deflection around the magnetosphere [Palmroth et al., 2003]. However, depending on which criterion is used to define the magnetopause (and the bow shock), the exact position of the boundary thus defined can vary significantly, as the different criteria are not met at exactly the same position [Palmroth et al., 2018, Battarbee et al., 2020]. We have added some clarification regarding the determination of the boundary positions at lines 184-187.

As discussed at lines 364-370 of the initially submitted manuscript, the main consequence of the 2D set-up is the enhanced piling-up of the field lines in front of the magnetopause. This results in a slow expansion of the bow shock and compression of the magnetopause. Therefore, the magnetosheath thickness is somewhat overestimated in the later times of our runs. However, this should not affect the global magnetosheath parameters, except near the magnetopause where the pile-up takes place. In the revised manuscript, we have elaborated on the 2D effects in the discussion (lines 434-436).

- Scales: could the authors give information on the temporal and spatial scales resolved in the simulations? And compare them to typical scales like inertial lengths and typical periods (inverses

of plasma/cyclotron frequencies). How does this compare with the 150s used for averaging magnetosheath parameters? This would help the interpretation of density variability mentioned 1289 for instance.

The spatial resolution is 300 km in Run 1 and 228 km in Runs 2A and 2B. The ion inertial length in the solar wind is 228 km in all three runs, which means that we have 1 cell/ion inertial length in Runs 2A and 2B, and 1.3 cell/ion inertial length in Run 1. This resolution is sufficient to resolve ion kinetic processes in a hybrid-Vlasov simulation (see Pfau-Kempf et al., 2018, and our response to Reviewer #1).

The ion cyclotron period in the solar wind is 13 s (Runs 1 and 2A) or 6.5 s (Run 2B). In the magnetosheath, their values are even smaller because of the larger magnetic field strength. The ion plasma period is about 50 ms in the solar wind in all three runs. The 150 s averaging interval used in our study is thus significantly larger than both typical periods, and the variability of the density cannot be linked with the ion gyroperiod for example.

In the revised manuscript, we have added the values of these typical temporal and spatial scales and compared them with the averaging interval (lines 157-162, 175-177, 204-206).

- Set-up: it is not clear to me why run 1 is set up in the XZ plane and arguments are sought for to justify it mimics correctly the XY plane. Why not using a proper set up in the XY plane from the start?

We agree with the reviewer that having all three simulations in the equatorial plane would have been ideal for our study. However, global hybrid-Vlasov simulations are computationally expensive. The runs presented here required from a few million to over 10 million CPU-hours to be carried out. For this study, we decided to make use of the already existing catalogue of Vlasiator simulations that was available to us, and which included runs with upstream conditions that were appropriate for the comparative study we are presenting. Since the different simulation planes are not critical with respect to the magnetosheath properties (provided that the cusp regions are carefully excluded, as we did in Run 1), running a new simulation was not deemed necessary for the present study.

We have added a mention to the computational cost of the simulations in Section 2.1 (lines 171-173), to make it clearer why we use a run in the XZ plane.

- Observations: for comparing observations and simulations the same statistical methodology should be employed, i.e. median or average for both, contrary to what is done in the paper.

Thank you for pointing out this lack of consistency, we should indeed have used the same statistical measure to quantify the “global” value of the asymmetry in each run. In the revised manuscript, we will give the range of values for each asymmetry, rather than the median or the mean which are problematic due to the large variations from bin to bin (see our response to the first point of Reviewer #2 for more detail).

Minor points:

- 195: ‘warranted’. Do the authors mean ‘mandatory’?

We will change the wording to “better suited” (line 109).

- Figure 1: mismatch between central / outer legends and d and e labels.

We will correct this, thank you for noticing the mismatch.

- 1400: smaller

We will correct the typo.

- 1427: 'statistical'. Do the authors refer to observations here?

Yes, this refers to the observations. We have reformulated this sentence to clarify this (line 516).

Additional references (not previously included in the manuscript bibliography)

Burgess, D.: Foreshock-shock interaction at collisionless quasi-parallel shocks, *Advances in Space Research*, 15, 159, doi:10.1016/0273-1177(94)00098-L, 1995.

Palmroth, M., Pulkkinen, T. I., Janhunen, P., & Wu, C.-C.: Stormtime energy transfer in global MHD simulation, *Journal of Geophysical Research (Space Physics)*, 108, 1048, doi:10.1029/2002JA009446, 2003.

Pfau-Kempf, Y., Battarbee, M., Ganse, U., Hoilijoki, S., Turc, L., von Alfthan, S., Vainio, R., & Palmroth, M.: On the importance of spatial and velocity resolution in the hybrid-Vlasov modeling of collisionless shocks, *Frontiers in Physics*, 6, 44, doi:10.3389/fphy.2018.00044, 2018.

Response to Reviewer #4

We thank the referee for their positive evaluation of our manuscript and for providing constructive remarks. Please find below our point-by-point response in bold font.

The paper studies asymmetry in the Earth's dayside magnetosheath using global hybrid-Vlasov simulations and compares numerical results with a statistical dataset of THEMIS observations. The paper is clearly written and the results are new and interesting. However, some details about modeling are missed. I partly agree with the comments of three other reviewers and mention several important points from their reports below. I could recommend the paper for publication after major revision.

Major remarks

1. Although the Vlasiator model is well known and I believe it has been thoroughly described in the literature, the paper should provide more details on the runs under discussion. In particular, (as also mentioned by one of the reviewers) the paper says nothing about spatial resolution. It would be useful to compare the resolution with the ion inertial length and gyroradius. The authors have already answered this issue in their reply to Reviewer 1 and I suppose it will appear in the paper too. The paper does not describe the simulation domains in each case; it only mentions that their size is different between the runs. I would be also curious to know what happens if the simulated intervals in Runs 2A and 2B would be increased since now they are shorter than in Run 1.

In Run 1, the simulation box extends from -48.6 to $64 R_E$ in the x direction and from -59.6 to $39.2 R_E$ in the z direction. In Runs 2A and 2B, it extends from -7.9 to $46.8 R_E$ in the x direction and between $\pm 31.3 R_E$ in the y direction. We have added the simulation domain extents, as well as more information regarding the spatial resolution, at lines 157-162 and 175-178.

Our Vlasiator runs comprise two phases. First, in the initialisation phase, the near-Earth magnetic environment forms self-consistently due to the interaction of the dipole field with the incoming solar wind. Then, the run continues in an almost steady state. Due to the 2D set-up of our runs, we never reach a completely steady state because the IMF piles up in front of the magnetopause, causing a slow expansion of the bow shock. In simulations including the foreshock on the dayside, as is the case for the three runs presented here, the main parameter which determines when a run is stopped is when foreshock waves reach the $+x$ boundary, as extending the simulation would likely cause unphysical wave reflection. As concerns the magnetosheath properties, we do not expect significant changes if Runs 2A and 2B were to be extended, except for a larger magnetosheath thickness, due to the field line pile-up.

We now mention that the simulations have reached a quasi-steady state in the interval under study (lines 220-221).

2. Both the Reviewers 1 and 3 noted that comparison with MHD runs for exactly the same solar wind conditions will be useful because this would emphasize which variations in the magnetosheath downstream of the quasi-parallel bow shock are essentially kinetic structures and cannot be predicted by MHD models. However, I do not think that it is necessary to run all MHD models available from CCMC, but it would be enough to make three runs with at least one model (e.g. SWMF/BATSRUS).

While we agree with the reviewer that an in-depth comparison of magnetosheath asymmetries in MHD and kinetic simulations would be an interesting topic of research, we feel that such a study lies beyond the scope of the present paper, as was also noted by Reviewer #3. Identifying the source of discrepancies between different numerical models is not trivial, as many factors can come into play, such as the spatial and temporal resolution, the numerical solvers being used, and so on. Even among MHD models, significant differences are observed, as shown for

example by Gordeev et al. [2015], who compared the outputs of the different MHD models available at CCMC.

Our paper presents a comprehensive and self-contained analysis of a set of three hybrid-Vlasov simulations complemented with spacecraft observations, which allow us to draw firm conclusions regarding the effects of several solar wind parameters. Whenever possible, we compared our results with MHD theory and with the MHD simulation results presented in Walsh et al. [2012] and Dimmock et al. [2013], and found them to be in good qualitative agreement. The only apparent discrepancy with MHD theory was the variation of the asymmetry level as a function of the Alfvén Mach number. However, when revisiting those results once the standard deviation of the asymmetry levels was taken into account, based on the suggestion from Reviewer #2, we found that the variation was not conclusive, and thus did not contradict MHD theory (see our response to the third major point of Reviewer #3). We have amended this paragraph (formerly at lines 295-300, now 358-366) when revising the manuscript. For these reasons, we feel that the present paper does not call for an extensive comparison with MHD simulations.

3. I also note that the solar wind conditions in the hybrid simulations are different from the typical solar wind conditions at L1. I am satisfied with the author's reply to Reviewer 1 that the Mach numbers in the solar wind stay in the typical interval and therefore the bow shock-magnetosheath properties may not be changed in comparison with those in observations. However, I would emphasize that the solar wind density of 1 cm^{-3} is significantly smaller than the average in observations (usually between 5 and 10 cm^{-3}). I think the paper should clearly explain this because I guess that the low solar wind density may be a reason for the stronger fluctuations in the magnetosheath than those in the data.

In the same manner as the high solar wind speed would not influence our results because of the typical Mach numbers in our simulations, the low density should not affect the bow shock-magnetosheath properties either, because the density compression ratio stays within its typical range at Earth. The low solar wind density does not result in large uncertainties in the density in our simulation because the hybrid-Vlasov formalism allows to describe accurately low density plasma, even in regions as tenuous as the magnetotail lobes. This low density does not affect either the development of wave activity in the magnetosheath, which is home to mirror modes [Hoilijoki et al., 2016] and EMIC waves [Dubart et al., 2020].

It would be helpful if the reviewer could provide us with a reference regarding the influence of solar wind density on the variability of magnetosheath properties, as it is not clear to us which other physical processes this could affect. This would be an interesting item to add to the discussion.

4. Since the authors use average parameters both in the simulations and observations, I think it would be possible to add standard deviations to the figures, e.g. in the form of error bars. This would be helpful when comparing the differences between the runs (how significant is the difference with respect to the standard deviations). Besides, the authors mention in the text that they calculated longer time average intervals (line 290). How long are they and does this make any difference to their conclusions?

Thank you for this suggestion. In the revised manuscript, we have added error bars to the asymmetry plots (line plots in Figures 1, 3, 6 and 7). As done in Dimmock et al. [2017], we estimate the error on the magnetosheath parameters as the standard error of the mean (standard deviation divided by the square root of the size of the bin sample). We then use this error to calculate the minimum and maximum values of the asymmetry in each bin, which determines the extent of the error bars in the asymmetry plots. The estimation of the error is described at lines 210-212 and 226-228.

We performed time averages over 50 s, 100 s and 150 s. We did not find any significant differences in the results we obtained. While the exact value of the asymmetry level varied in each bin (especially for the density), the polarity of the asymmetry remained identical, and the range of the asymmetry level over the whole magnetosheath was essentially unchanged. We have added explicitly the duration of the interval on which the averaging was performed to remove the ambiguity in this sentence (lines 352-353).

Minor remarks

1. The bibliography list in the paper is long, but I would like to mention two more papers, Zwan and Wolf (<https://doi.org/10.1029/JA081i010p01636>) who first mentioned the plasma depletion layer and Samsonov et al. (<https://doi.org/10.1029/2000JA900150>) who compared magnetosheath profiles downstream of the parallel and perpendicular bow shock using the anisotropic MHD model.

Thank you for these references, we have add them in the introduction.

2. Line 83. “These processes would thus favour the quasi-parallel flank.” But the results in the paper show the Qperp-favoured velocity asymmetry. How is this consistent?

Our results focus on the bulk velocity, which is larger in the quasi-perpendicular magnetosheath. In contrast, the studies of Dimmock et al. [2016a] and Nykyri et al. [2017] show that velocity fluctuations in the Pc 3 range (22 – 100 mHz) are stronger on the quasi-parallel flank and are favourable to the development of the Kelvin-Helmholtz instability. The difference in bulk velocity between the quasi-parallel and quasi-perpendicular flanks is probably not large enough to counteract the effect of the larger velocity fluctuations in the quasi-parallel sector, as it has been shown that the Kelvin-Helmholtz instability is more frequently observed on the quasi-parallel flank [Henry et al., 2017]. We have extend this paragraph of the introduction (lines 93-98) and added the reference to the study by Henry et al. [2017].

3. Lines 149-152. The figures in the paper show that the spatial bins are asymmetric with respect to the Sun-Earth line. Please, explain how this asymmetry is taken into account if you use the same shape as Shue et al.’s model which is symmetrical.

We used a different flaring parameter for the outer magnetosheath boundary on the quasi-parallel and quasi-perpendicular flank, to account for the different magnetosheath thicknesses. We have added an explanation for this in the revised manuscript (lines 191-192).

4. Caption to Figure 2. Please, define θ_{Bn} .

We have added the definition of θ_{Bn} in the figure caption.

5. Lines 233-235. Is θ_{Bn} equal to 0° and 90° near the terminator plane?

Yes. We have reformulate this sentence to better clarify this (lines 293-294).

6. Lines 265-266. I think it is better ”density compression ratio” instead of ”shock compression ratio”.

We agree that “density compression ratio” is less ambiguous. We have corrected this in the revised manuscript.

7. Label on Figure 5 says that the lines correspond to runs 1 & 2A and 2B but this contradicts the text (lines 265-266).

The text mentions only Runs 2A and 2B, as they are the two runs under discussion at this point in the text. We have added a mention to Run 1 as well to make it clear that the caption and the text are consistent with each other (lines 323-324).

8. Figure 4. The author may add an arrow to indicate the stagnation point.

Thank you for this suggestion. We have added a dashed line in Figure 4 to highlight where the Sun-Earth line is, which shows well that the minima of the velocity curves are shifted towards the quasi-parallel flank.

9. Lines 367-369. Is it better to say about an increase in the magnetic field on the quasi-perpendicular flank than about a decrease on the quasi-parallel flank?

This sentence refers to the low magnetic field strength downstream of the quasi-parallel shock, which remains equally low in the central magnetosheath as in the outer magnetosheath when the cone angle is reduced to 30° . In contrast, the magnetic field strength is higher in the central magnetosheath than in the outer magnetosheath for a 45° cone angle in Run 1 (see Figure 1a and 1b). On the quasi-perpendicular flank, the magnetic field strength is also lower in Run 2A than in Run 1 because of the lower θ_{Bn} value due to the more radial IMF orientation. The field line draping does not cause an increase of the magnetic field strength on the quasi-perpendicular flank in this run. We have reformulated this sentence to clarify this (lines 439-442).

Additional references (not previously included in the manuscript bibliography)

Dubart, M., Ganse, U., Osmane, A., Johlander, A., Battarbee, M., Grandin, M., Pfau-Kempf, Y., Turc, L., and Palmroth, M.: Resolution dependence of magnetosheath waves in global hybrid-Vlasov simulations, *Ann. Geophys. Discuss.*, <https://doi.org/10.5194/angeo-2020-24>, in review, 2020.

Gordeev, E., Sergeev, V., Honkonen, I., Kuznetsova, M., Rastätter, L., Palmroth, M., Janhunen, P., Tóth, G., Lyon, J., & Wiltberger, M.: Assessing the performance of community-available global MHD models using key system parameters and empirical relationships, *Space Weather*, 13, 868, doi:10.1002/2015SW001307, 2015.

Hoilijoki, S., Palmroth, M., Walsh, B. M., Pfau-Kempf, Y., von Alfthan, S., Ganse, U., Hannuksela, O., & Vainio, R.: Mirror modes in the Earth's magnetosheath: Results from a global hybrid-Vlasov simulation, *Journal of Geophysical Research (Space Physics)*, 121, 4191, doi:10.1002/2015JA022026, 2016.

Henry, Z. W., Nykyri, K., Moore, T. W., Dimmock, A. P., & Ma, X.: On the Dawn-Dusk Asymmetry of the Kelvin-Helmholtz Instability Between 2007 and 2013, *Journal of Geophysical Research (Space Physics)*, 122, 11,888, doi:10.1002/2017JA024548, 2017.

Changes made in the manuscript

Abstract:

- A few sentences have been added to better highlight the novelty of our results.
- Quasi-parallel shock effects are now mentioned together with foreshock effects.

Introduction:

- We have added references suggested by the reviewers.
- Magnetopause processes are now mentioned as a source of asymmetries for high energy particles.
- We have added a paragraph presenting previous works using kinetic simulations.

Methodology:

- We now mention how the plasma moments are calculated from the distribution functions in the simulations.
- Additional information regarding the run parameters is provided (spatial resolution, extent of the spatial domain, Mach numbers, typical temporal scales, etc).
- We provide more details regarding the boundary determination for the magnetosheath binning.
- We describe how the error on the magnetosheath parameters and the asymmetries is estimated.
- We have added a new paragraph at the end of the section to clarify our approach and its validity.

Results:

- We removed the mention of the average or the median value of the asymmetry across all azimuthal bins, as it wasn't well representative of the global asymmetry level, and replaced it with the asymmetry level range. This changes in particular the results concerning the density asymmetry, as we now conclude that it does not vary notably from one run to the other.
- We clarified the values of the θ_{bn} angle near the terminator in Run 1.
- We compare the magnetosheath densities we obtained with previous numerical results.

Discussion:

- We discuss the effects of the quasi-parallel shock in addition to the foreshock effects.
- We have extended the discussion on possible 2D effects in the simulation.
- We have included a paragraph discussing the spatial resolution in the simulation.
- We have reformulated some sentences to better convey our meaning.

Conclusions:

- We have added a few sentences to better highlight the novelty of our results.
- We have reformulated some sentences to better convey our meaning.

Figures:

- We have added error bars on Figures 1, 3, 6 and 7
- We have corrected the outer magnetosheath asymmetry in Run 1 (Figures 1e, 3e and 6e) after fixing an error in our analysis program.
- We have added labels to indicated the quasi-parallel and quasi-perpendicular sides and a vertical dashed line in Figure 4.

In addition to the changes requested by the reviewers, we would like to note that we have corrected the results of Run 1 in the outer magnetosheath, as we found an error in the outer boundary parameters, which explained the very irregular density and velocity profiles for this run. This did not change any significant conclusions.

- We modified the discussion on the velocity asymmetry (Section 3.2) based on the updated results
- As a result, we removed from the conclusions the statement that the velocity asymmetry fluctuations are reduced when the Mach number is lower, as this is not shown anymore on the updated figure.
- We modified the description of the density asymmetry in Run 1 accordingly. This did not change any conclusion of the study.

Asymmetries in the Earth's dayside magnetosheath: results from global hybrid-Vlasov simulations

Lucile Turc¹, Vertti Tarvus¹, Andrew Dimmock², Markus Battarbee¹, Urs Ganse¹, Andreas Johlander¹, Maxime Grandin¹, Yann Pfau-Kempf¹, Maxime Dubart¹, and Minna Palmroth^{1,3}

¹Department of Physics, University of Helsinki, Helsinki, Finland

²IRF-U, Uppsala, Sweden

³Finnish Meteorological Institute, Helsinki, Finland

Correspondence: Lucile Turc (lucile.turc@helsinki.fi)

Abstract. Bounded by the bow shock and the magnetopause, the magnetosheath forms the interface between solar wind and magnetospheric plasmas and regulates solar wind-magnetosphere coupling. Previous works have revealed pronounced dawn-dusk asymmetries in the magnetosheath properties. The dependence of these asymmetries on the upstream parameters remains however largely unknown. One of the main sources of these asymmetries is the bow shock configuration, which is typically quasi-parallel on the dawn side and quasi-perpendicular on the dusk side of the terrestrial magnetosheath because of the Parker spiral orientation of the interplanetary magnetic field (IMF) at Earth. Most of these previous studies rely on collections of spacecraft measurements associated with a wide range of upstream conditions which are processed in order to obtain average values of the magnetosheath parameters. In this work, we use a different approach and quantify the magnetosheath asymmetries in global hybrid-Vlasov simulations performed with the Vlasiator model. We concentrate on three parameters: the magnetic field strength, the plasma density and the flow velocity. We find that the Vlasiator model reproduces accurately the polarity of the asymmetries, but that their level tends to be higher than in spacecraft measurements, probably because the magnetosheath parameters are obtained from a single set of upstream conditions in the simulation, making the asymmetries more prominent. **A set of three runs with different upstream conditions allows us to investigate for the first time** how the asymmetries change when the angle between the IMF and the Sun-Earth line is reduced and when the Alfvén Mach number decreases. We find that a more radial IMF results in a stronger magnetic field asymmetry and a larger variability of the magnetosheath density. In contrast, a lower Alfvén Mach number leads to a reduced magnetic field asymmetry and a decrease in the variability of the magnetosheath density, the latter likely due to weaker foreshock processes. Our results highlight the strong impact of the **quasi-parallel shock and its associated foreshock** on global magnetosheath properties, in particular on the magnetosheath density, which is extremely sensitive to transient **quasi-parallel shock** processes, **even with the perfectly steady upstream conditions in our simulations. This could explain the large variability of the density asymmetry levels obtained from spacecraft measurements in previous studies.**

Copyright statement.

1 Introduction

The interaction of the supermagnetosonic solar wind with the Earth's magnetosphere forms a standing bow shock which decelerates the incoming flow to submagnetosonic speeds in front of the obstacle. Extending between the bow shock and the magnetopause, the magnetosheath houses shocked solar wind plasma, which has been compressed and heated at the shock crossing. **It is home to intense low-frequency wave activity, predominantly due to the mirror mode and the Alfvén ion cyclotron mode (e.g. Schwartz et al., 1996; Génot et al., 2009; Soucek et al., 2008).** At the interface between the solar wind and the magnetosphere, the magnetosheath regulates the processes which transfer momentum and energy from the former to the latter and thus plays a key role in solar wind-magnetosphere coupling (Pulkkinen et al., 2016; Eastwood et al., 2017). Understanding and accurate modelling of this coupling therefore call for an in-depth knowledge of magnetosheath properties and their dependence on upstream solar wind parameters.

Since the early gasdynamic model of Spreiter et al. (1966), the magnetosheath has been subject to intensive scrutiny (e.g. Petrinec et al., 1997; Paularena et al., 2001; Longmore et al., 2005; Lucek et al., 2005; Dimmock and Nykyri, 2013; Lavraud et al., 2013; Dimmock et al., 2017). These studies revealed that the magnetosheath properties display significant spatial variations, as a function of the distance from the boundaries, with for example the formation of the plasma depletion layer near the magnetopause during northward interplanetary magnetic field (IMF) conditions (e.g. Zwan and Wolf, 1976; Wang et al., 2004), and as a function of the distance from the Sun-Earth line, with pronounced dawn-dusk asymmetries (see the reviews by Walsh et al., 2014; Dimmock et al., 2017, and references therein). One of the main sources of these dawn-dusk asymmetries is the bow shock, **another one being the leakage of magnetospheric particles into the magnetosheath, which result in a dawn-dusk asymmetry of the energetic ion and electron components in the magnetosheath plasma (Anagnostopoulos et al., 2005; Cohen et al., 2017).** **In this paper, we concentrate on the impact of the bow shock properties on the large-scale distribution of the magnetosheath properties.**

The shock properties depend strongly on the angle θ_{Bn} between the IMF and the local normal to the shock's surface. Because of the Parker-spiral orientation of the IMF at Earth, which makes a 45° angle with the Sun-Earth line, the dusk side of the magnetosheath generally lies downstream of a quasi-perpendicular (Q_\perp) shock ($\theta_{Bn} > 45^\circ$), while the dawn side is associated with a quasi-parallel (Q_\parallel) shock ($\theta_{Bn} < 45^\circ$). Even in the fluid approximation, these contrasted shock regimes result in different plasma properties in the downstream region. Using the Rankine-Hugoniot jump conditions, Walters (1964) found larger plasma densities and temperatures downstream of the quasi-parallel shock than downstream of the quasi-perpendicular shock. Global magnetohydrodynamic (MHD) simulations have brought additional support to the dawn magnetosheath being home to a hotter and denser plasma, while the magnetic field strength and flow velocity are larger on the dusk flank (Samsonov et al., 2001; Walsh et al., 2012).

Investigating magnetosheath asymmetries using spacecraft measurements is a challenging task because it requires an extensive spatial coverage of this region. Since simultaneous measurements in different parts of the magnetosheath are scarce, most observational studies rely on compilations of spacecraft observations from different passes through this region to build statistical maps of the magnetosheath properties (Paularena et al., 2001; Němeček et al., 2002; Longmore et al., 2005; Walsh

et al., 2012; Dimmock and Nykyri, 2013). The main drawbacks of this approach are that these data are collected during vastly different upstream conditions and that the position of the spacecraft relative to the magnetosheath boundaries is essentially unknown. The former issue is generally addressed by normalising the magnetosheath parameters with their solar wind counterparts, while empirical models of the magnetosheath boundaries provide an estimate of the relative position of the spacecraft inside the magnetosheath.

Consistent with the aforementioned theoretical and numerical works, observational studies have reported a dusk-favoured asymmetry of the magnetic field strength and of the plasma velocity (Longmore et al., 2005; Walsh et al., 2012; Dimmock and Nykyri, 2013; Dimmock et al., 2017). The ion temperature, on the other hand, showcases a dawn-favoured asymmetry, probably due to enhanced heating at the more turbulent quasi-parallel shock (Walsh et al., 2012; Dimmock et al., 2015a). Furthermore, magnetic field and velocity fluctuations are stronger in the dawn magnetosheath (Dimmock et al., 2014, 2016a), while temperature anisotropy and mirror mode wave activity are more prominent in the dusk sector (Dimmock et al., 2015b; Soucek et al., 2015). **In an earlier study by Tátrallyay and Erdős (2005), no dawn-dusk asymmetry was evidenced for mirror mode occurrence, but it should be noted that the data were not organised according to the shock configuration in this work, contrary to the more recent studies by Dimmock et al. (2015b) and Soucek et al. (2015).**

The density asymmetry turned out to be more elusive in spacecraft measurements. Though a clear dawn-favoured asymmetry was found in several data sets (Paularena et al. (2001) for solar maximum; Němeček et al. (2002); Walsh et al. (2012); Dimmock et al. (2016b)), others did not display any significant asymmetry levels (Dimmock and Nykyri, 2013; Paularena et al., 2001, for solar minimum), or even an asymmetry with a changing polarity depending on the location inside the magnetosheath (Němeček et al., 2003; Longmore et al., 2005). We note that because they originate from different spacecraft missions, the data sets used in these studies cover various parts of the magnetosheath: nightside (Paularena et al., 2001), close to the terminator (Němeček et al., 2002, 2003), dayside at high latitudes (Longmore et al., 2005), and dayside near the equatorial plane, either near the magnetopause (Walsh et al., 2012; Dimmock et al., 2016b) or across the whole magnetosheath thickness (Dimmock and Nykyri, 2013). They also correspond to various parts of the solar cycle, which may affect the level of the density asymmetry because the average solar wind parameters depend on solar activity. However, opposite behaviours were reported by Paularena et al. (2001) and Dimmock et al. (2016b).

The dependence of magnetosheath asymmetries on upstream parameters can bring insight into the processes that create them. Longmore et al. (2005) and Dimmock et al. (2017) found no clear dependence of the density and velocity asymmetries on the IMF direction, suggesting that they may not be driven by the bow shock. On the other hand, the level of these asymmetries increases with the Alfvén Mach number (M_A), as does the temperature asymmetry, according to the numerical simulations performed by Walsh et al. (2012). They also show that an increasing M_A would also tend to increase the magnetic field strength asymmetry. Walsh et al. (2012) ascribe the observed density asymmetry to the asymmetric bow shock shape, as its quasi-parallel sector lies closer to the magnetopause than its quasi-perpendicular sector. They argue that the apparent lack of dependence of the density asymmetry on the IMF direction in statistical studies is likely due to the limited number of data points associated with non-Parker-spiral IMF orientations. As evidenced by these contradicting claims, many open questions

remain regarding the precise sources of the observed magnetosheath asymmetries and their dependence on upstream solar wind conditions.

Asymmetries in the magnetosheath parameters result in turn in an asymmetric magnetospheric driving. **Large amplitude velocity fluctuations in the magnetosheath are conducive to a faster growth of the Kelvin-Helmholtz instability at the Earth’s magnetopause and larger plasma transport through the boundary (Nykyri et al., 2017). Such velocity fluctuations are stronger in the quasi-parallel magnetosheath (Dimmock et al., 2016a), and these, accompanied with the lower tangential field strength in this region, result in the Kelvin-Helmholtz instability favouring the quasi-parallel flank (Henry et al., 2017).** Also, ions of magnetosheath origin in the plasma sheet present a dawn-favoured asymmetry of about 30 – 40% (Wing et al., 2005). This asymmetry could partially be explained by the temperature asymmetry in the magnetosheath, while additional heating processes may be regulated by the asymmetric distribution of other magnetosheath parameters (Dimmock et al., 2015a; Dimmock et al., 2017).

Numerical simulations can help shed new light onto magnetosheath asymmetries, as they provide a global view of the magnetosheath for a given set of solar wind conditions, instead of relying on statistical maps constructed from measurements associated with a variety of upstream parameters. This also removes possible errors when determining the context of magnetosheath measurements, which must be combined with time-lagged data from an upstream monitor in observational studies. To date, most numerical studies of magnetosheath asymmetries have used MHD models (Walsh et al., 2012; Dimmock and Nykyri, 2013), though the temperature asymmetry was qualitatively compared with the outputs from a hybrid-Particle-in-Cell simulation by Dimmock et al. (2015a). The physics of the quasi-parallel bow shock and its associated foreshock are however inherently kinetic in nature, and thus a kinetic approach is **better suited** to study magnetosheath parameters downstream of the quasi-parallel shock.

Hybrid-kinetic simulations, that is, including ion kinetic effects but where electrons are treated as a fluid, are extensively used to study the interaction of the solar wind with planetary magnetospheres, and in particular foreshock, bow shock and magnetosheath processes (e.g. Omidi et al., 2005; Lin and Wang, 2005; Blanco-Cano et al., 2006; Omidi et al., 2014; Karimabadi et al., 2014; Turc et al., 2015; Modolo et al., 2018; Palmroth et al., 2018). A number of numerical studies of the magnetosheath focus on wave activity in this region and the competition between mirror modes and Alfvén ion cyclotron waves (e.g., Trávníček et al., 2007; Herčík et al., 2013; Hoilijoki et al., 2016). The numerical simulations of Omidi et al. (2014) revealed large-scale filamentary structures in the quasi-parallel magnetosheath, while Karimabadi et al. (2014) investigated small-scale processes such as turbulence and reconnection.

In this paper, we present the first analysis of magnetosheath asymmetries as obtained from global ion kinetic simulations performed with the hybrid-Vlasov model Vlasiator (von Alfvén et al., 2014; Palmroth et al., 2018). We use a set of three different runs to investigate the effects of the IMF cone angle θ_{Bx} (measured between the IMF vector and the Sun-Earth line) and the solar wind Alfvén Mach number, which are key parameters controlling the shock properties. In this first study based on hybrid-Vlasov simulations, we choose to focus on three primary magnetosheath parameters: the magnetic field strength B , the plasma velocity V and the ion density n_p . For the latter, we will attempt to identify possible reasons for its large variability in observational studies.

Table 1. Summary of the run parameters

Run name	Simulation plane	Δr [km]	IMF cone angle $\theta_{B,x}$	IMF strength [nT]	M_A	n_{SW} [cm^{-3}]	\mathbf{V}_{SW} [km s^{-1}]
Run 1	$x - z$ plane	300	45°	5	6.9	1	$(-750, 0, 0)$
Run 2A	$x - y$ plane	227	30°	5	6.9	1	$(-750, 0, 0)$
Run 2B	$x - y$ plane	227	30°	10	3.5	1	$(-750, 0, 0)$

2 Methodology

2.1 The Vlasiator simulation

Vlasiator is a hybrid-Vlasov model designed to perform global simulations of the Earth’s plasma environment while retaining ion kinetic physics (von Alfthan et al., 2014; Palmroth et al., 2018). In the hybrid-Vlasov formalism, ions are treated as velocity distribution functions evolving in phase space whereas electrons are modelled as a cold massless charge-neutralising fluid. The temporal evolution of the system is obtained by solving Vlasov’s equation, coupled with Maxwell’s equations. Ohm’s law, including the Hall term, provides closure to the system. In Vlasiator, the use of realistic proton mass and charge, together with the full strength of the Earth’s dipole field, results in processes being simulated at their actual physical scales, as encountered in near-Earth space. This makes the comparison with spacecraft measurements straightforward.

The runs presented in this paper are two-dimensional (2D) in ordinary space. Each grid cell in ordinary space is self-consistently coupled with a 3D velocity space in which the ion distribution functions evolve. **In each ordinary space cell, the plasma parameters are obtained as the moments of the velocity distribution function, by integration over the velocity space.** The coordinate system used in the simulation is equivalent to the Geocentric Solar Ecliptic (GSE) reference frame. In this Earth-centred frame, the x -axis points towards the Sun, z is perpendicular to the Earth’s orbital plane and points northward, and y completes the right-handed triplet. Depending on the runs, the simulation domain covers either the equatorial ($x - y$) or the noon-midnight meridional ($x - z$) plane (see Table 1 for a summary of the run parameters). In equatorial runs, we use the Earth’s magnetic dipole with its actual value of $8.0 \times 10^{22} \text{ A m}^2$, while for runs in the noon-midnight meridional plane, a 2D line dipole is used (Daldorff et al., 2014). In all runs, the solar wind flows into the simulation domain from the $+x$ edge. Copy conditions are applied at the other walls of the simulation domain, while periodic conditions are employed for the out-of-plane cell boundaries (i.e., in the z direction for a run in the $x - y$ plane). The inner boundary of the simulation domain is a circle at about $4.7 R_E$ from the Earth’s centre, considered a perfect conductor.

2.2 Runs used

In this study, we analyse three Vlasiator runs, each corresponding to different IMF conditions (see Table 1). This allows us to investigate the influence of the IMF orientation and strength (and by extension the Alfvén Mach number) on magnetosheath asymmetries. In all three runs, the solar wind ions are injected at the inflow boundary as a Maxwellian population with a density

$n_{\text{SW}} = 1 \text{ cm}^{-3}$ and a temperature $T_{\text{SW}} = 0.5 \text{ MK}$, flowing at a velocity $\mathbf{V}_{\text{SW}} = (-750, 0, 0) \text{ km s}^{-1}$, thus corresponding to fast solar wind conditions.

In the reference run, hereafter Run 1, the IMF vector makes a 45° cone angle with the Sun-Earth line and lies in the $x - z$ plane, with $\mathbf{B} = (3.54, 0., -3.54) \text{ nT}$. **This results in an Alfvén Mach number $M_A = 6.9$ and a magnetosonic Mach number $M_{\text{ms}} = 5.5$, which fall inside the range of typical values for these Mach numbers at Earth (Winterhalter and Kivelson, 1988).** Therefore, despite the large solar wind speed in our runs, we have a typical density compression ratio at the bow shock with our input parameters. The simulation domain extends from -48.6 to $64.3 R_E$ ($R_E = 6371 \text{ km}$) in the x direction and from -59.6 to $39.2 R_E$ in the z direction. The spatial resolution in this run is $\Delta r = 300 \text{ km}$, that is, 1.3 solar wind ion inertial length ($d_i = 227.7 \text{ km}$), and the velocity space resolution is 30 km/s . In a hybrid-Vlasov simulation, these resolutions are sufficient to resolve the dominant ion kinetic processes in the foreshock-bow shock-magnetosheath system (see Hoilijoki et al., 2016; Pfau-Kempf et al., 2018; Dubart et al., 2020). Possible limitations due to the chosen resolutions are discussed in Section 4.

Run 1 simulates the noon-midnight meridional plane of near-Earth space, as it was initially designed to study e.g. dayside and nightside reconnection in the presence of the foreshock (Hoilijoki et al., 2019). For an Alfvénic Mach number $M_A = 6.9$ as in Run 1, the quasi-perpendicular portion of the bow shock lies roughly at the same distance from Earth both in the $x - y$ and the $x - z$ planes, while its quasi-parallel sector is found closer to Earth, according to MHD simulations (Chapman et al., 2004). Therefore, if the IMF lies in the $x - z$ plane, the position and shape of the bow shock in this plane are essentially the same as those observed in the equatorial plane for an IMF vector in the $x - y$ plane. Since the main parameter controlling most magnetosheath asymmetries is the bow shock configuration (Dimmock et al., 2017), the IMF configuration in Run 1 is roughly equivalent to a Parker spiral IMF orientation in the equatorial plane in terms of bow shock and outer magnetosheath properties (i.e. away from the cusps and the reconnecting magnetopause). **Although this setup is not ideal, it is sufficient for the purpose of the present study, and we deemed that running a new simulation was not warranted, as Vlasov runs are computationally expensive, requiring of the order of several million CPU-hours.** We will use this run as a reference for the most typical IMF orientation at Earth.

The other set of two runs, Runs 2A and 2B, are equatorial runs, with a 30° cone angle IMF in the $x - y$ plane. **In both Runs 2A and 2B, the simulation box extends from -7.9 to $46.8 R_E$ in the x direction and between $\pm 31.3 R_E$ in the y direction. The spatial resolution is $\Delta r = 227 \text{ km}$, that is, 1 solar wind ion inertial length, and the velocity space resolution is 30 km/s .** In Run 2A, the IMF strength is set to 5 nT , as in Run 1, while in Run 2B, its value is set to 10 nT . As a result, the Alfvén Mach number M_A is reduced to 3.5 in this run, half of its value in Runs 1 and 2A where $M_A = 6.9$. To avoid confusion in the case where the simulation plane is not the equatorial plane, we will refer to the polarity of the magnetosheath asymmetries as Q_\perp -favoured or Q_\parallel -favoured, instead of the dawn-dusk terminology generally used in observational studies.

2.3 Analysis method

In each run, we divide the dayside magnetosheath into sectors within which we calculate the average magnetosheath properties, as illustrated by the black curves in Figure 1a. **Determining the exact bow shock and magnetopause positions proved to**

185 **be rather impractical, as their position can vary significantly depending on the parameter which is selected to define the boundary (Palmroth et al., 2018; Battarbee et al., 2020). Therefore, we decided to use a simpler method to define approximate boundaries that would serve as the inner and outer limits for our magnetosheath binning.** We use for simplicity the same shape as that of the Shue et al. (1997) magnetopause model (of the form $r = r_0(2/(1 + \cos\theta))^\alpha$), where r_0 is the stand-off distance, θ the angle from the Sun-Earth line and α the flaring parameter, to delineate the boundaries of the bins
190 in the radial direction. This shape approximates relatively well the bow shock and magnetopause shape in our simulations when different flaring parameters are used. **For the bow shock, we also use a different flaring parameter for the quasi-parallel and the quasi-perpendicular flanks, to account for the asymmetric bow shock shape.**

For each run, the values for $r_0 = r_{\min}$ (inner boundary), $r_0 = r_{\max}$ (outer boundary) and α are selected by visual inspection so as to maximise the coverage of the magnetosheath while remaining sufficiently far from the bow shock and the magne-
195 topause to avoid including data from other regions. The two intermediate radial boundaries are placed at one third and two thirds of the magnetosheath thickness $r_{\max} - r_{\min}$. We denote the relative position between the magnetosheath boundaries as $F_{\text{Msheath}} = (r - r_{\min}) / (r_{\max} - r_{\min})$. In the azimuthal direction, the magnetosheath is divided into 18 10° -wide angular bins. In our analysis, we will only focus on the central and outer sets of radial bins, to ensure that the cusps are excluded and that magnetopause processes do not affect our results in Run 1.

200 Inside each of these bins, we calculate the average values of various magnetosheath parameters, namely the ion density, the plasma bulk velocity and the magnetic field strength. In addition to spatial averages within each bin, we also perform temporal averages in order to minimise the effects of transient features originating from the foreshock or arising inside the magnetosheath. Here we use 150 s temporal averages to calculate the magnetosheath parameters, which was found as a good trade-off to remove the effect of transients with only limited changes in the position of the magnetosheath boundaries. **This**
205 **averaging interval is much larger than the proton gyroperiod in the solar wind (13 s in Runs 1 and 2A and 6.5 s in Run 2B), and is comparable with the 180 s window used by Dimmock et al. (2017) for spacecraft measurements. We also calculated the median value of the magnetosheath parameters within each bin, for the same spatial and temporal sample, and we obtained very similar results. To facilitate the comparison with the most recent studies of magnetosheath asymmetries (Dimmock et al., 2017, and references therein), which are based on average values, we present here the results obtained**
210 **from averaging the magnetosheath parameters. As in Dimmock et al. (2017), we estimate the error associated with each parameter within each bin as the standard error of the mean, $SEM = \sigma / \sqrt{N}$, where σ is the standard deviation and N is the number of simulation cells inside each bin.**

We note here that because of the 2D set-up of our simulations, field lines tend to pile-up at the magnetopause, as they cannot slip along the magnetosphere flanks. As a result, the bow shock moves slowly outwards. To ensure that the comparison of
215 the different runs is meaningful, we select time intervals in Run 1 and Run 2A when the bow shock shape was comparable, as it should not be strongly affected by the different IMF cone angles. In Run 1, we calculate the average magnetosheath parameters between $t = 700$ and $t = 850$ s, when the simulation has properly initialised and before the onset of intense dayside reconnection, which could cause changes in the flow pattern near the magnetopause, and to limit the effects of reconnection-driven magnetic islands in the magnetosheath (Pfau-Kempf et al., 2016). In Runs 2A and 2B, we use the interval from $t = 350$

220 to $t = 500$ s. The initialisation phase of these runs is shorter than in Run 1 because of their smaller simulation domain. **At these times, all three runs have reached a quasi-steady state.**

Following Dimmock et al. (2017), we define the asymmetry of the magnetosheath parameters as:

$$A = 100 \times \left(\frac{Q_{\perp} - Q_{\parallel}}{Q_{\perp} + Q_{\parallel}} \right) \quad (1)$$

where Q_{\perp} is the average value of a magnetosheath parameter (here magnetic field strength, plasma velocity or ion density) in a given azimuthal and radial bin in the quasi-perpendicular magnetosheath, and Q_{\parallel} its average value in the corresponding opposite bin, i.e., symmetric with respect to the Sun-Earth line, in the quasi-parallel magnetosheath. **The error of the asymmetry is estimated as the extreme values of A when injecting $Q_{\perp} \pm SEM$ and $Q_{\parallel} \pm SEM$ into Eq. 1 (see Dimmock et al., 2017).** Note that we use the same arrangement of quasi-perpendicular and quasi-parallel bins in the analysis of Runs 2A and 2B, even though the reduced cone angle in these runs shifts the transition between the two shock regimes away from the bow shock nose. This facilitates the comparison with observational studies, which do not account for the IMF cone angle in their mapping of the magnetosheath parameters (e.g. Dimmock et al., 2017).

We also note here that although the simulation input parameters deviate from average values in the solar wind at Earth, this is not an issue for the comparison with previous observational studies. The statistical data sets, based on compilations of magnetosheath measurements associated with a wide variety of solar wind conditions, rely on the assumption that magnetosheath parameters can be normalised to their solar wind counterparts to obtain the average distribution of magnetosheath properties. In the present work, the normalisation of the data to the solar wind quantities together with the typical shock Mach numbers and compression ratio in our simulations ensure that the comparison with spacecraft observations is meaningful.

3 Results

240 3.1 Magnetic field strength

Colour-coded in the top panels of Figure 1 is the magnetic field strength in the dayside magnetosheath and the neighbouring regions, normalised to the IMF strength, in each of the three runs. As indicated by the magnetic field lines (light grey curves), the quasi-parallel sector of the bow shock and its associated foreshock extend in the lower part of each plot, upstream of the southern ($z < 0$, in Run 1) or dawnside ($y < 0$, in Runs 2A and 2B) magnetosheath. The colour scheme is chosen to highlight the areas of the magnetosheath where the normalised magnetic field strength is above or below 4, which is the upper limit for the magnetic field compression at the bow shock crossing according to the Rankine-Hugoniot jump conditions (Treumann, 2009). In Run 2B, the normalised magnetic field strength is below 4 in most of the magnetosheath, due to the weaker compression at the bow shock when the Alfvén Mach number is low. In Runs 1 and 2A, it remains below 4 in the first few R_E downstream of the subsolar bow shock, and in a much broader area in the flank magnetosheath. In regions closer to the magnetopause, its values increase well above 4 due to the field lines piling up in front of the magnetosphere. In the subsolar region, the effects of pile-up are visible even in the outermost magnetosheath bins used in our study (black curves), while they are limited

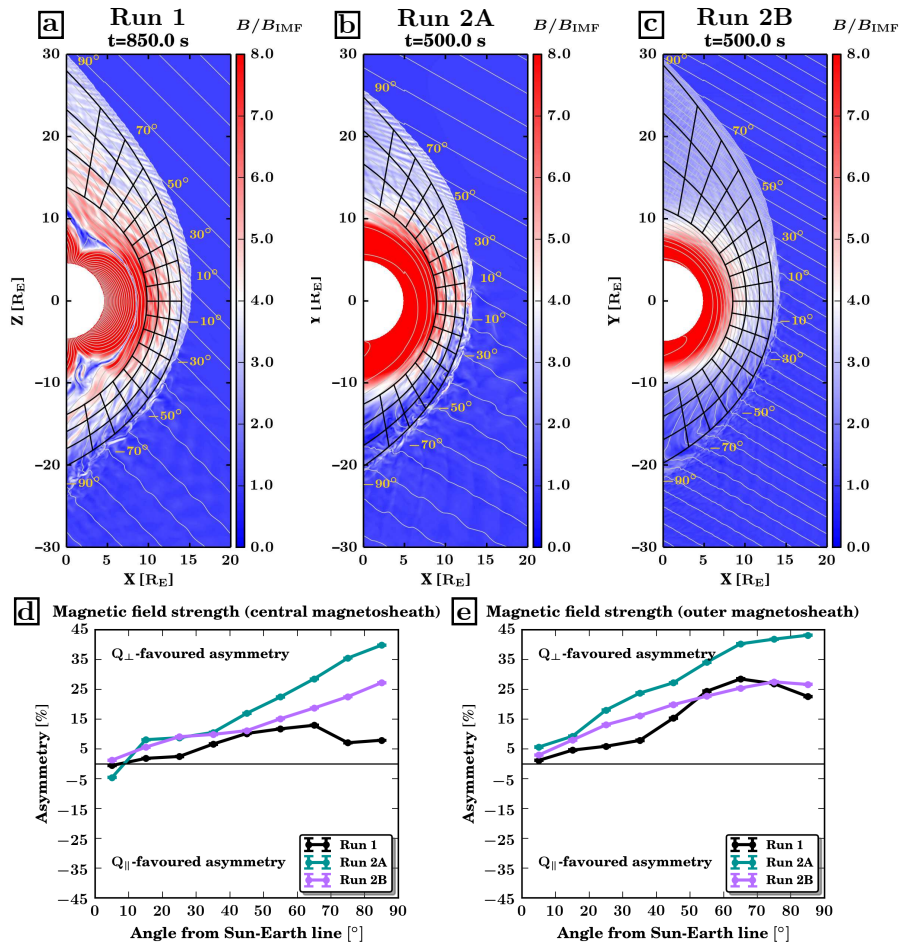


Figure 1. Top panels: magnetic field strength in the simulation plane, normalised with the IMF strength, in Run 1 at time $t = 850$ s (a), in Run 2A (b) and 2B (c) at time $t = 500$ s. The light grey lines show magnetic field lines. The spatial bins used to calculate the average magnetosheath parameters are shown in black. Bottom panels: magnetic field strength asymmetry in the central (d) and outer (e) magnetosheath. The error bars are obtained from the extreme values of the asymmetry based on the standard error of the mean in each bin (see Section 2.3).

to the central and inner magnetosheath bins further on the flanks. They also extend further out in the quasi-perpendicular magnetosheath than downstream of the quasi-parallel shock, due to the IMF orientation. Similar features due to pile-up are also observed in the statistical maps compiled by Dimmock et al. (2017) (see the top panels of their Figure 5.1). The only significant difference between our simulation results and Dimmock et al. (2017)'s maps is the large magnetic field strength along the northern magnetopause close to the terminator in Run 1, which is likely due to the 2D set-up of our simulation, resulting in enhanced field line pile-up. In the following, we will exclude from our analysis the innermost magnetosheath bins and concentrate on the central and outer magnetosheath properties.

The bottom panels of Figure 1 show the asymmetry (see Eq. 1) of the magnetic field strength in the central ($1/3 < F_{\text{Msheath}} < 2/3$) and outer ($2/3 < F_{\text{Msheath}} < 1$) magnetosheath as a function of the angle from the Sun-Earth line. The asymmetry level is obtained from both a spatial average of this parameter inside each azimuthal bin and a temporal average over 150 s of the simulation, in order to minimise the effects of transient structures in the magnetosheath. **The error bars associated with the asymmetry are very small compared to those from spacecraft observations (e.g. Dimmock et al., 2017), most likely due to the steady upstream conditions in our runs and the large number of simulation cells in each spatial bin.** Figures 1d and e reveal a definite Q_{\perp} -favoured asymmetry (positive values of the asymmetry) in all three runs. In Run 1, which corresponds to a typical Parker-spiral IMF orientation at Earth, we find an **asymmetry level ranging between 0 and 15% in the central magnetosheath.** The asymmetry level is significantly larger just downstream of the shock, suggesting that the field line draping and pile-up in front of the magnetosphere tend to smooth out the effects of the bow shock. Our results are in good agreement with the 0–10% Q_{\perp} -favoured asymmetry obtained by Dimmock et al. (2017) based on statistics of spacecraft data. This Q_{\perp} -favoured asymmetry is due to the stronger compression of the magnetic field at the quasi-perpendicular bow shock, because only the tangential magnetic field components are enhanced at the bow shock crossing, while the normal component remains unchanged (Treumann, 2009; Hoilijoki et al., 2019).

When the cone angle is reduced from 45° to 30° in Runs 2A and 2B, the asymmetry becomes stronger in the central magnetosheath, exceeding 40% on the flanks in Run 2A. This is most likely due to the quasi-parallel sector of the shock being shifted closer to the subsolar point, and thus affecting a larger fraction of the dayside magnetosheath. As a result, the regions of very low magnetic field strength (in dark blue in the bottom parts of panels a-c), due to the weak magnetic field compression at the quasi-parallel shock crossing, extend over most of the dawn side magnetosheath, forming a starker contrast with the dusk sector. We also note that they penetrate deeper in the magnetosheath, resulting in similar levels of magnetic field asymmetry in the outer and the central magnetosheath in Runs 2A and 2B. This contrast between Run 1 and Runs 2A and 2B may be related to the different draping pattern of the field lines at lower cone angle.

The magnetic field asymmetry is significantly weaker in Run 2B than in Run 2A. This lower asymmetry level at lower M_A is most likely due to the reduced magnetic field compression affecting more strongly the magnetic field strength downstream of the quasi-perpendicular bow shock. To confirm this, we calculate the magnetic field strength just downstream of the bow shock based on the Rankine-Hugoniot jump conditions and assuming magnetic coplanarity is satisfied. We use the solar wind parameters of the Vlasiator runs as upstream conditions. The downstream to upstream ratio of the magnetic field magnitude is displayed in Figure 2 as a function of θ_{Bn} and M_A . This clearly shows that the magnetic field compression at the quasi-parallel bow shock does not vary with M_A for the considered M_A range, while higher values are reached on the quasi-perpendicular side as M_A increases. These different behaviours on the quasi-parallel and the quasi-perpendicular sectors as a function of M_A result in a less pronounced asymmetry at lower M_A .

Finally, we observe a gradual increase in the asymmetry from the subsolar region towards the flanks. This is likely due to the variation of the θ_{Bn} angle along the bow shock surface. In Run 1, θ_{Bn} increases from the bow shock nose to the terminator on the quasi-perpendicular side, while it decreases at a similar rate on the quasi-parallel side, reaching its extrema on both flanks in the last azimuthal bin near the terminator. **We have $\theta_{\text{Bn}} \sim 0^{\circ}$ ($\theta_{\text{Bn}} \sim 90^{\circ}$) near the terminator on the quasi-parallel (quasi-**

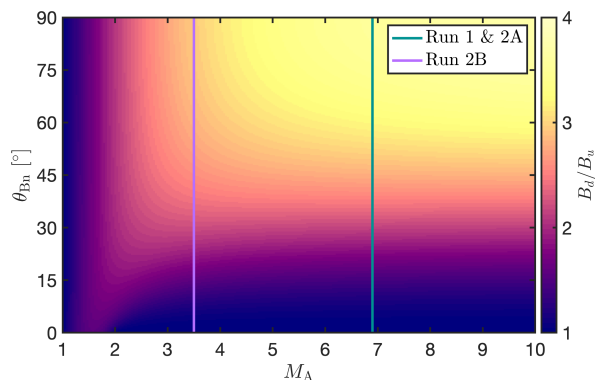


Figure 2. Downstream to upstream ratio of the magnetic field strength as a function of the Alfvén Mach number M_A and the θ_{Bn} between the IMF direction and the shock normal, calculated based on the Rankine-Hugoniot relations.

perpendicular) flank. In Runs 2A and 2B, θ_{Bn} also increases with the azimuthal angle on the quasi-perpendicular side, but on the quasi-parallel sector, it first decreases until reaching 0 at around 45° from the Sun-Earth line, and then starts increasing again. The magnetic field asymmetry keeps increasing beyond this point probably because the asymmetry level is computed in a broad area and not just in the close vicinity of the bow shock, and other effects than shock compression come into play in the magnetosheath, for example field line pile-up and draping around the magnetosphere.

3.2 Ion bulk velocity

Figure 3 displays the plasma bulk velocity normalised to the solar wind speed in the three runs, and its associated asymmetry in the central and outer magnetosheath, in the same format as Figure 1. Again, the asymmetry is calculated based on a 150 s average of the bulk velocity inside each of the magnetosheath bins. As expected, the plasma velocity is very low in the subsolar magnetosheath, while the flow is faster on the flanks, because the tangential velocity is mostly preserved at the shock while its normal component is reduced, according to Rankine-Hugoniot relations.

Figure 3d shows a pronounced Q_\perp -favoured asymmetry in the central magnetosheath, **with an asymmetry level ranging between 10 and 20% in Run 1 and in Run 2B.** In Run 2A, very high values, over 25%, are reached in some azimuthal bins close to the subsolar region, but **the overall asymmetry level appears only marginally higher than in the other runs.** Dimmock and Nykyri (2013) and Dimmock et al. (2017) evidenced a Q_\perp -favoured asymmetry in their statistical data set, albeit with values somewhat below those found in our simulations, between 0 and 10%. Walsh et al. (2012) also reported a velocity asymmetry with the same polarity in spacecraft measurements and in MHD simulations.

In the outer magnetosheath, the level of the asymmetry tends to decrease when moving away from the subsolar region, **except in the last two azimuthal bins in Run 1.** As illustrated in Fig. 4, which shows the average velocity in the outer magnetosheath as a function of the angle from the Sun-Earth line, the flow speed increases more rapidly on the quasi-parallel flank than on the quasi-perpendicular flank. This progressively smoothes out the difference between both sectors. Also, the fact that the velocity

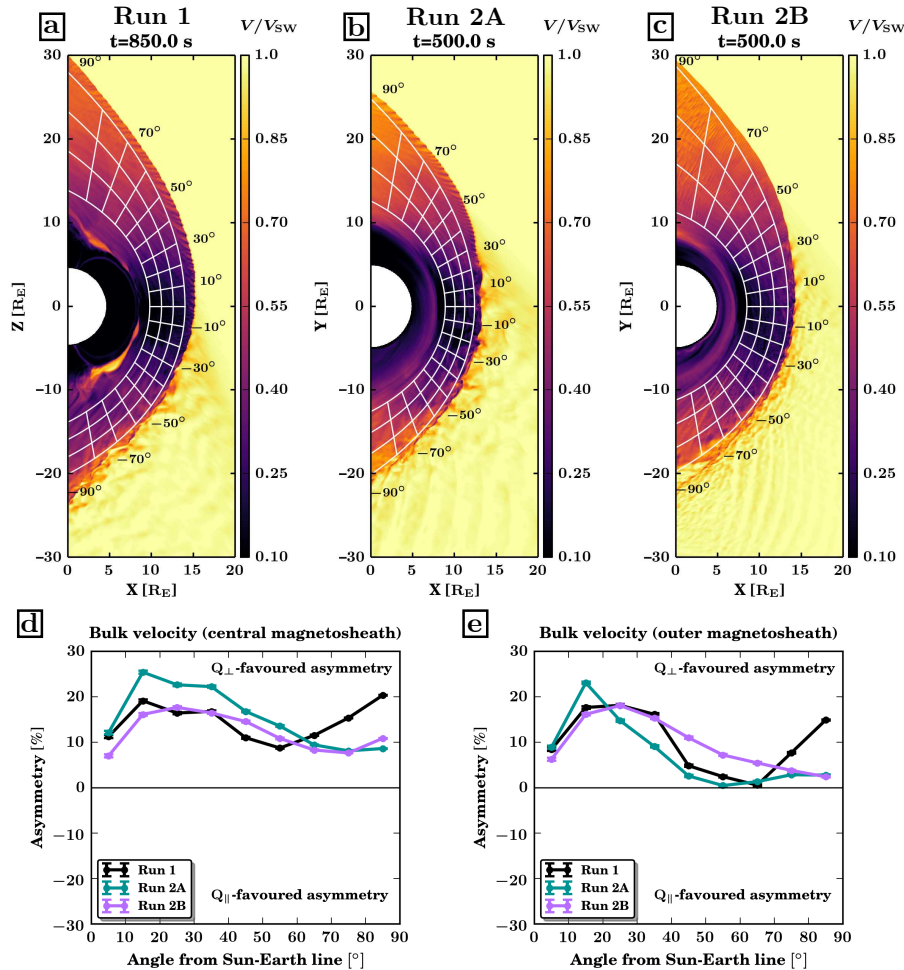


Figure 3. Top panels: ion bulk velocity in the simulation plane, normalised with the solar wind speed, in Run 1 at time $t = 850$ s (a), in Run 2A (b) and 2B (c) at time $t = 500$ s. The spatial bins used to calculate the average magnetosheath parameters are shown in black. Bottom panels: magnetic field strength asymmetry in the central (d) and outer (e) magnetosheath.

315 is larger further down on the flanks tends to reduce the asymmetry level, as the same absolute difference in velocity between the quasi-parallel and quasi-perpendicular sectors results in a smaller value of the asymmetry, which is calculated as the relative difference (see Eq. 1).

Beyond 40° from the Sun-Earth line, the asymmetry level reduces to values close to 0 in Run 2A and partly in Run 1. Only in Run 2B does the asymmetry remain persistently Q_\perp -favoured across the entire dayside magnetosheath. The re-increase of the asymmetry level in the last two azimuthal bins in Run 1 reflects an abrupt decrease in velocity near the terminator on the quasi-parallel flank. This likely stems from the irregular shape of the bow shock in Run 1, which bulges outward beyond -70° from the Sun-Earth line due to a large and persistent foreshock transient.

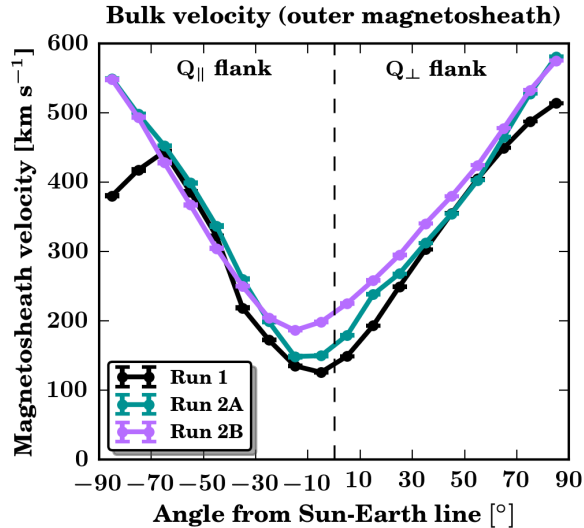


Figure 4. Bulk velocity in the outer magnetosheath as a function of the angle from the Sun-Earth line in all three runs.

Figure 5 displays the shock **density** compression ratio as a function of θ_{Bn} for the two different M_A values in **Runs 1 and 2A** ($M_A = 6.9$) **and in Run 2B** ($M_A = 3.5$). As illustrated in Fig. 5, the **density** compression ratio is roughly constant over the whole θ_{Bn} range for the M_A of Runs 1 and 2A (in green), while it is considerably lower on the quasi-perpendicular side than on the quasi-parallel side at the lower M_A of Run 2B (in purple). **This could explain why the velocity asymmetry level is essentially larger in Run 2B than in Run 2A in the outer magnetosheath (Fig. 3e). This trend however disappears deeper in the magnetosheath (Fig. 3d), probably because other processes affect there the magnetosheath flow.**

Our simulations also show that the flow stagnation region is slightly shifted from the subsolar point towards the quasi-parallel magnetosheath (see Fig. 4 **where the dashed line indicates the subsolar point**). In Run 1, the velocity minimises at about 10° from the Sun-Earth line on the quasi-parallel side. This is probably due to the velocity deflection at the bow shock which depends on θ_{Bn} , as predicted by the Rankine-Hugoniot jump conditions to preserve the continuity of the tangential electric field (e.g., Treumann, 2009). As a result, asymmetric flow speeds are observed when comparing the quasi-perpendicular and quasi-parallel magnetosheath. Field line draping around the magnetosphere may also play a role in reducing the velocity in the quasi-parallel magnetosheath. The shift of the stagnation region towards the quasi-parallel flank is slightly greater for a 30° cone angle (Runs 2A and 2B), consistent with the θ_{Bn} dependence of the velocity deviation at the bow shock.

3.3 Ion density

Plotted in Fig. 6 is the ion density and its associated asymmetry in the central and outer magnetosheath, in the same format as Figures 1 and 3. The upper panels show that the ion density in the magnetosheath is essentially up to four times its upstream value, consistent with previous works and with the theoretical density compression ratio at the bow shock (Formisano et al.,

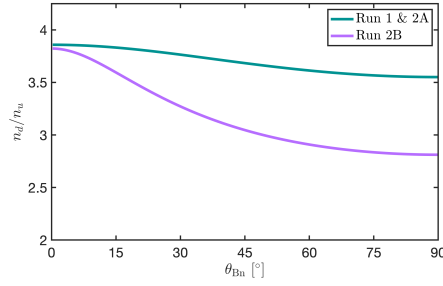


Figure 5. Density compression ratio as a function of θ_{Bn} for two different M_A values, corresponding to those in the simulation runs.

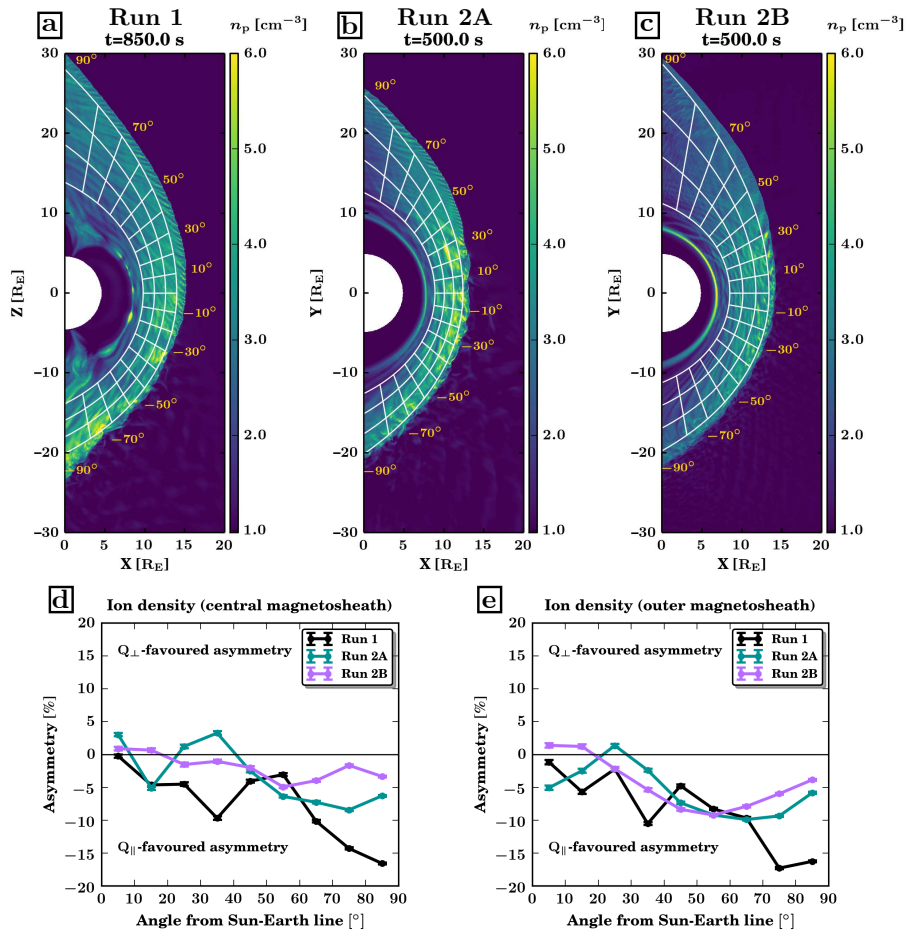


Figure 6. Same format as in Figure 3 but for the ion density.

1973). A few regions of larger density enhancements (in yellow) are observed downstream of the quasi-parallel shock. Similar transient density enhancements are seen throughout the 150 s of simulated time which are used to calculate the magnetosheath

asymmetry. **Such large densities in the magnetosheath, exceeding the theoretical MHD limit, are a common feature in hybrid-kinetic simulations of the bow shock/magnetosheath system (see for example Omidi et al., 2014; Karimabadi et al., 2014). They are probably due to density enhancements in the foreshock which are advected and compressed through the bow shock, and appear to be associated with ripples of the shock front.**

Figures 6d and 6e evidence a mostly Q_{\parallel} -favoured asymmetry of the ion density in the magnetosheath. **However, in Runs 2A and 2B, associated with a 30° cone angle, multiple azimuthal bins near the subsolar region display an opposite polarity of the asymmetry, both in the outer and the central magnetosheath.** Moreover, we note that the values of the density asymmetry are much more sensitive to the time interval over which the data are averaged than for the other parameters under study. This is probably due to the variability of the plasma density just downstream of the quasi-parallel shock. The patches of high density alternate with depleted regions, which result in Q_{\perp} -favoured asymmetries in some azimuthal bins, even when performing 150 s temporal averages. This demonstrates the high variability of the magnetosheath density, even under completely steady solar wind conditions. For example, in Run 2A, we note that patches of high density just downstream of the bow shock are concentrated in the subsolar magnetosheath and are distributed on either sides of the Sun-Earth line, as evidenced in Figure 6b. This could explain the reversed polarity of the asymmetry in some azimuthal bins near the subsolar point.

The asymmetry levels appear to be essentially similar when comparing the different runs. The Q_{\parallel} -favoured asymmetry might be more pronounced near the terminator in Run 1 than in the other runs, but the large fluctuations of the asymmetry level from one bin to another makes it difficult to ascertain. As mentioned in Section 3.2, the shock compression ratio shows little dependence on θ_{Bn} in the range of M_A associated with Runs 1 and 2A, while it is significantly lower on the quasi-perpendicular flank than on the quasi-parallel flank in the low M_A range, such as in Run 2B. Therefore, according to the MHD theory, the density asymmetry should be stronger at lower M_A . **We do not observe however a significant variation of the asymmetry level between Runs 2A and 2B, possibly due to the spatial variability of the magnetosheath density, or to the low cone angle value. The flatter shape of the bow shock at lower M_A would also tend to counteract the effect of the density compression ratio, as only a smaller range of θ_{Bn} values is found at the surface of a more planar bow shock.**

Finally, we note that the variability of the density in the outer magnetosheath is much lower at reduced M_A , which results in a smoother distribution of the asymmetry. This could be related to foreshock disturbances being weaker at lower M_A , since the density of suprathermal ions is reduced (Turc et al., 2015, 2018).

3.4 Comparison with spacecraft observations

We now compare our numerical results with the asymmetries obtained from a statistical data set of magnetosheath observations from the Time History of Events and Macroscale Interactions during Substorms (THEMIS) spacecraft (Angelopoulos, 2008; Dimmock and Nykyri, 2013; Dimmock et al., 2017). The data were collected between January 2008 and December 2017 and are binned according to the spacecraft coordinates in the Magnetosheath InterPlanetary Medium (MIPM) reference frame (Bieber and Stone, 1979; Dimmock et al., 2017). In this coordinate system, the x -axis points opposite to the solar wind flow, while the y -axis is defined such that the quasi-perpendicular sector of the bow shock lies in the $+y$ direction and its

quasi-parallel sector at negative y . This ensures that all data associated with a given shock regime are grouped together on one side of the magnetosheath. The z -axis completes the orthogonal set. Then the radial coordinate of each measurement point is calculated as the fractional distance between a model bow shock and magnetopause, which removes the effects of the motion of these boundaries due to changing upstream conditions. The data points are thus organised with their fractional distance inside a normalised magnetosheath and with their azimuthal angle from the Sun-Earth line. Each measurement point is associated with a set of upstream conditions, based on the OMNI data (King and Papitashvili, 2005) at the time of the THEMIS observations. More details on the data processing can be found in Dimmock and Nykyri (2013); Dimmock et al. (2017) and the references therein.

As in previous studies using this statistical data set (e.g. Dimmock et al., 2015a; Dimmock et al., 2017), we concentrate only on measurements in the central magnetosheath, that is, where $1/3 < F_{\text{Msh}} < 2/3$, to avoid including data from other regions in case of inaccuracies in the determination of the boundary position. The average parameters in the central magnetosheath are computed inside 15° -wide angular bins, with a 50% overlap between two consecutive bins. The asymmetry is then calculated using Eq. 1. Furthermore, we divide the statistical data set into two ranges of cone angles, depending on the IMF orientation associated with each of the magnetosheath measurements. The magnetosheath asymmetries associated with a cone angle close to that of the Parker spiral orientation ($40^\circ < \theta_{\text{Bx}} < 50^\circ$) are shown in black in Figure 7 and those associated with a lower cone angle value ($20^\circ < \theta_{\text{Bx}} < 35^\circ$) are plotted in blue. We note here that the data set contained too few data points at $M_A < 5$ for us to investigate the change in the asymmetries at low Alfvén Mach number.

Firstly, we find an excellent agreement between simulations and observations regarding the polarity of the asymmetry for the three parameters considered here, as noted already in the previous sections. The levels of asymmetry tend however to be lower in the observational data compared to the simulations. This could be due to the processing method of the statistical data set, which calculates averages over very diverse upstream conditions, and thus results in a conservative estimate of the asymmetry.

As concerns the influence of the cone angle, the statistical data do not show evidence of a significant increase in the magnetic field strength asymmetry when the cone angle is reduced, contrary to our numerical simulations. The density asymmetry displays much more spatial variability at low cone angle, with about half of the azimuthal bins having a Q_\perp -favoured asymmetry, while most of them showed a clear Q_\parallel -favoured asymmetry for a Parker spiral IMF orientation. This agrees well with the numerical results presented above, and is likely due to foreshock processes causing enhanced variability of the magnetosheath density at lower cone angles.

4 Discussion

We have quantified the asymmetry of the magnetic field magnitude, ion density and bulk flow velocity inside the dayside magnetosheath in three Vlasiator global runs with different IMF conditions. We note that the use of global **ion-kinetic** simulations presents **several** main advantages.

First, the global coverage of the magnetosheath for a given set of solar wind conditions provided by the simulations allows us to investigate the asymmetries both in the central and the outer magnetosheath. In contrast, observational studies are

410 often restricted to the central magnetosheath to make sure that the data set does not include magnetosphere or solar wind
measurements (e.g. Dimmock et al., 2015a; Dimmock et al., 2017), or to locations just outside the magnetopause to avoid
relying on boundary models to estimate the position inside the magnetosheath (Walsh et al., 2012). **The comparison of the
asymmetry levels in the central and outer magnetosheath provides us with new information regarding the influence of
the bow shock on the magnetosheath parameters, in particular on the magnetic field asymmetry, which is stronger just
415 downstream of the shock than deeper in the magnetosheath.**

Second, the simulations enable us to investigate the asymmetry levels at low Alfvén Mach number ($M_A \sim 3.5$, Run 2B),
while the statistical data set compiled from THEMIS measurements does not contain enough data points at such low M_A to
derive the asymmetry of the magnetosheath parameters. This is why we did not compare our numerical results concerning M_A
with observations in Section 3.4. Low Alfvén Mach numbers are encountered only occasionally at Earth, but they are of great
420 importance for solar wind-magnetosphere coupling because they are associated with extreme solar wind disturbances such as
magnetic clouds (Turc et al., 2016) and they result in atypical conditions in the magnetosheath (Lavraud and Borovsky, 2008;
Lavraud et al., 2013). Other studies have suggested that the Alfvén Mach number plays a role in the asymmetry (Walsh et al.,
2012; Dimmock et al., 2017) but it is difficult to make a direct and meaningful comparison between all of these studies since
there are extensive differences across methodologies, models, and datasets. However, there are clearly unanswered questions
425 which deserve further study and may be addressed with future missions and/or model runs.

**Third, the inclusion of ion kinetic physics in the simulations makes it possible to study the effects of the quasi-parallel
shock and its associated foreshock on magnetosheath parameters. These effects are particularly substantial for the ion
density, whose variability in the magnetosheath is driven by quasi-parallel bow shock and foreshock processes. The
alternating patches of higher and lower densities, which are chiefly responsible for the varying asymmetry levels in the
430 outer magnetosheath, appear to be associated with irregularities of the shock front, whose scale is comparable to that of
the foreshock waves, consistent with previous studies which have established that foreshock waves modulate the shape
of the shock front (e.g. Burgess, 1995).**

The main limitation of our numerical simulations is the 2D set-up, which results in particular in enhanced field line pile-up in
front of the magnetopause, and thus causes a slow outward motion of the bow shock. **Therefore, the magnetosheath thickness
435 is somewhat overestimated in the later times of our runs. However, this should not alter the global magnetosheath
parameters, except near the magnetopause where the pile-up takes place.** We verified that this does not affect significantly
the asymmetry levels, and found that the **temporal** variability of the asymmetries in the simulation was caused by transient
processes rather than by the shock progressive expansion. The 2D set-up may also influence the field line draping pattern
in the magnetosheath, **which may affect the extent of the region of low magnetic field strength observed in the central
440 magnetosheath downstream of the quasi-parallel shock when the cone angle is reduced to 30° . In contrast, the magnetic
field strength is higher in the central magnetosheath than in the outer magnetosheath for a 45° cone angle in Run 1 (see
Figure 1a and 1b).** Future 3D simulations could allow us to evaluate if the asymmetry is less pronounced in this region than
in the outer magnetosheath when field lines can flow around the magnetosphere.

Another possible limitation of our simulations is the spatial resolution, which corresponds to 1.3 solar wind ion
445 inertial lengths in Run 1 and 1 ion inertial length in Runs 2A and 2B. As a result, waves with a wavelength below this
spatial resolution are not included in our simulations. This resolution is however sufficient to resolve the dominant low-
frequency wave modes in the magnetosheath, namely the mirror and the Alfvén ion cyclotron waves (Hoilijoki et al.,
2016; Dubart et al., 2020). At the shock front, a cell size of 1 ion inertial length or larger may not correctly evaluate
the gradient in the ramp. However, the hybrid-Vlasov formalism based on distribution functions enables the use of a
450 slope limiter which allows for total variation diminishing evolution of discontinuities and steep slopes even at somewhat
lower resolution. The shock transition is therefore well described in our simulations, and the downstream parameters
are correctly modelled. The study we present here focuses on the large-scale distribution of magnetosheath properties.
Therefore, the spatial resolution in our Vlasiator runs is sufficient to study global magnetosheath parameters and how
they are impacted by ion kinetic physics.

455 We note that the levels of asymmetry obtained from the numerical simulations are larger than those from the observational
data set, for all parameters considered in this study. This is probably due to the fundamentally different methods through which
the magnetosheath parameters were obtained. In the simulations, the asymmetry is calculated based on spatial averages of
the magnetosheath parameters for a single set of steady upstream conditions, while observational results are a compilation
of localised measurements taken during a variety of upstream conditions. Specifically, the IMF can assume any orientation
460 in the observational data set, including in particular an out-of-plane component while the THEMIS spacecraft orbit near the
Earth’s equatorial plane. Even though the MIPM reference frame arranges the measurements corresponding to the quasi-
parallel/quasi-perpendicular sectors on the negative/positive y -hemispheres, it does not account for the different cone angles
nor for the out-of-plane IMF component. As a result, data points associated with widely different θ_{Bn} values can be grouped
together. Also, some data points may be misidentified as quasi-parallel or quasi-perpendicular because the upstream conditions
465 are determined from the OMNI propagated data set which may not reflect exactly the actual conditions at Earth’s bow shock.
These two effects would tend to smooth out the asymmetries in the statistical data set. The numerical simulations, on the other
hand, do not suffer from these limitations, resulting in more pronounced asymmetries. **A similar interpretation was proposed
by Walsh et al. (2012), who also found larger asymmetry levels in their MHD simulations than in the observations. This
further supports that** the apparent discrepancy between observations and simulations is only a natural consequence of the
470 different methods used for obtaining the average magnetosheath parameters.

The magnetic field asymmetry also behaves differently in the observations and the simulations when changing the cone
angle. In Vlasiator, we find a significant increase of the asymmetry at low cone angle, whereas **no significant variation is
observed** in the statistical THEMIS data set. It should be noted that the spacecraft observations are not associated with a single
value of the IMF cone angle, but are a compilation of measurements taken for a range of cone angles, between 20 and 35°.
475 As the IMF becomes more radial, the quasi-parallel sector of the bow shock and its associated foreshock move closer to the
subsolar point. For a purely radial IMF, the magnetosheath asymmetries due to the bow shock configuration should completely
disappear, as the θ_{Bn} values are then distributed symmetrically about the Sun-Earth line (see e.g. Turc et al., 2016). Therefore,
there should be a value of the cone angle at which the magnetosheath asymmetries maximise, before decreasing when further

reducing the cone angle to finally reach the symmetrical configuration for a purely radial IMF. The range of cone angles used
480 in collating the statistical data might therefore contain significant variation in asymmetry levels. This in turn could explain why
the asymmetry level for $20 - 35^\circ$ cone angles remains the same as for $40 - 50^\circ$ cone angles in the observations.

Using a semi-empirical model of the magnetosheath magnetic field (Turc et al., 2014), we calculate the asymmetry level
of the magnetic field strength associated with the same upstream parameters as in Run 1 and Run 2A. The model predicts a
higher asymmetry level at 30° than at 45° cone angle (not shown), in agreement with our numerical simulations. This lends
485 further support to the hypothesis that the different behaviour in spacecraft measurements could be due to the array of solar wind
conditions and IMF orientations included in the statistical data set. Also, the data could be affected by processes at smaller
spatial scales than those resolved in our simulations, though it is unlikely that this will play a significant role here, since the
data are averaged over several minutes.

The ion density asymmetry was essentially Q_{\parallel} -favoured in all our runs, consistent with previous observational and numerical
490 works (Paularena et al., 2001; Longmore et al., 2005; Walsh et al., 2012; Dimmock et al., 2016b) and MHD theory (Walters,
1964). It should be noted however that the most recent studies by Dimmock et al. (2016b) and Dimmock et al. (2017) only found
a clear Q_{\parallel} -favoured asymmetry near the magnetopause, while no clear polarity was observed in the central magnetosheath. In
our simulations, we found in several instances that the asymmetry in some of the azimuthal bins displayed an opposite polarity.
We also observed a large temporal variability of both its level and its polarity in our simulations, despite the completely steady
495 upstream conditions. This suggests that the magnetosheath density is extremely sensitive to transient processes, originating
for example in the foreshock **and at the quasi-parallel bow shock**. The fluctuations that are typically present in the solar
wind parameters would be conducive to even more variability of the magnetosheath density. The inconclusive results regarding
the polarity of this asymmetry in the central magnetosheath (Dimmock et al., 2016b; Dimmock et al., 2017) and the large
discrepancies in the asymmetry levels quantified in various studies (see the summary table in Walsh et al., 2014) likely stem
500 from this high variability.

5 Conclusions

In this work, we studied the asymmetry between the quasi-parallel and the quasi-perpendicular sectors of the Earth's magne-
tosheath using global hybrid-Vlasov simulations. We quantified the level of asymmetry in the central and outer magnetosheath
for the magnetic field strength, ion density and bulk velocity and investigated its variation when reducing the cone angle and
505 the M_A . For all parameters, we find a polarity of the asymmetry (Q_{\perp} -favoured or Q_{\parallel} -favoured) that is consistent with earlier
works (see Dimmock et al., 2017, for a recent review). The asymmetry levels tend to be higher in the numerical simulations,
due to the fact that the magnetosheath parameters are obtained for a given set of fixed upstream conditions in the model, instead
of a compilation of normalised localised measurements. **Using a set of three runs with different upstream conditions, we
investigated for the first time how the asymmetries change when the angle between the IMF and the Sun-Earth line is
510 reduced and when the Alfvén Mach number decreases.**

For a 30° cone angle, we found similar levels of magnetic field asymmetry in the outer and central magnetosheath, while they differed significantly at a larger cone angle. We also noted that the **polarity of the density asymmetry reversed in some bins near the subsolar region, likely due to the quasi-parallel sector of the bow shock being located closer to the subsolar point**. The magnetic field strength asymmetry increased significantly at 30° cone angle, possibly due to the low θ_{Bn} near the bow shock nose resulting in a reduced magnetic field compression across most of the quasi-parallel flank of the magnetosheath. This effect was however not observed in the statistical data sets **obtained from spacecraft measurements**.

Reducing the M_A results in a less pronounced magnetic field asymmetry because of the weaker compression of the magnetic field at the quasi-perpendicular bow shock, while that at the quasi-parallel shock remains roughly unchanged. We also noted that the density asymmetry displays less variability, probably due to weaker foreshock **and quasi-parallel shock** disturbances at lower M_A . This change is particularly visible here because of the low cone angle, but may be less discernable for less radial IMF orientations, as the foreshock will retreat towards the flank. Future simulation runs with a low M_A and a larger cone angle could allow to test this.

It is worth noting that even for completely steady upstream conditions, the magnetosheath density shows significant temporal and spatial variations, in particular downstream of the quasi-parallel shock. These variations are likely caused by foreshock **and quasi-parallel shock** transient processes. They can influence noticeably the level of asymmetry in some parts of the magnetosheath, and even cause reversals of its polarity in some azimuthal sectors. Our results show that density asymmetry variations in the magnetosheath are an inherent effect of the bow shock and foreshock, instead of a statistical artefact. This is most likely one of the sources for the wide variety of levels of density asymmetry quantified in previous observational studies.

This work shows that global kinetic simulations provide a reliable tool to study magnetosheath asymmetries. The global coverage of the magnetosheath obtained in each run allows for a precise quantification of the asymmetry levels for a given set of solar wind conditions, in contrast with spacecraft statistical data sets which quantify the average value of the asymmetries across a wide range of upstream conditions. Moreover, the inclusion of ion kinetic physics is necessary to properly describe **the dynamics of the quasi-parallel shock** which affect strongly the variability of the magnetosheath density. Numerical simulations also enable us to perform parametric studies, thus allowing us to study the influence of specific upstream parameters. Here we limited our analysis to three runs because of the large computational cost of Vlasiator simulations, but future studies could make use of larger sets of runs, with more varied upstream conditions, once they become available.

Code availability. Vlasiator (<http://www.helsinki.fi/en/researchgroups/vlasiator/>, Palmroth, 2020) is distributed under the GPL-2 open source license at <http://github.com/fmihpc/vlasiator/> (Palmroth and the Vlasiator team, 2020). Vlasiator uses a data structure developed in-house (<https://github.com/fmihpc/vlsv/>, Sandroos, 2019), which is compatible with the VisIt visualization software (Childs et al., 2012) using a plugin available at the VLSV repository. The Analysator software (<https://github.com/fmihpc/analysator/>, Hannuksela and the Vlasiator team, 2020) was used to produce the presented figures. The runs described here take several terabytes of disk space and are kept in storage maintained within the CSC – IT Center for Science. Data presented in this paper can be accessed by following the data policy on the Vlasiator web site.

Author contributions. L.T. initiated and coordinated the study, performed part of the data analysis and wrote the first draft of the manuscript.
545 V.T. developed the methodology and performed the initial data analysis. A.D. provided the THEMIS statistical data set and helped in the interpretation of the results. A.J. provided Figures 2 and 5, and contributed to the comparison with the Rankine-Hugoniot jump conditions. M.P. is the PI of the Vlasiator model and gave inputs to the interpretation of the simulation results. M.B., U.G. and Y.P.-K. ran the Vlasiator runs used in this study. Together with A.J., M.G. and M.D., they contributed to the analysis of the Vlasiator outputs. All co-authors participated in the discussion of the results and contributed to improving the manuscript.

550 *Competing interests.* The authors declare that they have no conflict of interest.

Acknowledgements. This project has received funding from the European Union’s Horizon 2020 research and innovation programme under the Marie Skłodowska-Curie grant agreement No 704681. The work of L.T. is supported by the Academy of Finland (grant number 322544). We acknowledge the European Research Council for Starting grant 200141-QuESpace, with which Vlasiator was developed, and Consolidator grant 682068-PRESTISSIMO awarded to further develop Vlasiator and use it for scientific investigations. The work leading to
555 these results has been carried out in the Finnish Centre of Excellence in Research of Sustainable Space (Academy of Finland grant numbers 312351 and 312390). V.T. acknowledges the Academy of Finland (grant number 328893) We acknowledge PRACE Tier-0 grant number 2016153521 with which Run 1 was carried out in CINECA, Italy. The CSC - IT Center for Science in Finland is acknowledged for the Grand Challenge awards leading to the results shown here for Runs 2A and 2B.

References

- 560 Anagnostopoulos, G. C., Vassiliadis, E. S., and Karanikola, I.: Dawn dusk asymmetry in spatial distribution and origin of energetic ion events upstream the Earth's bow shock, *Planetary and Space Science*, 53, 53–58, <https://doi.org/10.1016/j.pss.2004.09.028>, 2005.
- Angelopoulos, V.: The THEMIS Mission, *Space Sci. Rev.*, 141, 5–34, <https://doi.org/10.1007/s11214-008-9336-1>, 2008.
- Battarbee, M., Ganse, U., Pfau-Kempf, Y., Turc, L., Brito, T., Grandin, M., Koskela, T., and Palmroth, M.: Non-locality of Earth's quasi-parallel bow shock: injection of thermal protons in a hybrid-Vlasov simulation, *Annales Geophysicae*, 38, 625–643, 565 <https://doi.org/10.5194/angeo-38-625-2020>, 2020.
- Bieber, J. W. and Stone, S. C.: Energetic electron bursts in the magnetopause electron layer and in interplanetary space., in: *Magnetospheric Boundary Layers*, edited by Battrick, B., Mort, J., Haerendel, G., and Ortner, J., vol. 148 of *ESA Special Publication*, pp. 131–135, 1979.
- Blanco-Cano, X., Omidi, N., and Russell, C. T.: Macrostructure of collisionless bow shocks: 2. ULF waves in the foreshock and magnetosheath, *Journal of Geophysical Research (Space Physics)*, 111, A10205, <https://doi.org/10.1029/2005JA011421>, 2006.
- 570 Burgess, D.: Foreshock-shock interaction at collisionless quasi-parallel shocks, *Advances in Space Research*, 15, 159–169, [https://doi.org/10.1016/0273-1177\(94\)00098-L](https://doi.org/10.1016/0273-1177(94)00098-L), 1995.
- Chapman, J. F., Cairns, I. H., Lyon, J. G., and Boshuizen, C. R.: MHD simulations of Earth's bow shock: Interplanetary magnetic field orientation effects on shape and position, *Journal of Geophysical Research (Space Physics)*, 109, A04215, <https://doi.org/10.1029/2003JA010235>, 2004.
- 575 Childs, H., Brugger, E., Whitlock, B., Meredith, J., Ahern, S., Pugmire, D., Biagas, K., Miller, M., Harrison, C., Weber, G. H., Krishnan, H., Fogal, T., Sanderson, A., Garth, C., Bethel, E. W., Camp, D., Rübél, O., Durant, M., Favre, J. M., and Navrátil, P.: VisIt: An End-User Tool For Visualizing and Analyzing Very Large Data, in: *High Performance Visualization—Enabling Extreme-Scale Scientific Insight*, pp. 357–372, Chapman & Hall / CRC, 2012.
- Cohen, I. J., Mauk, B. H., Anderson, B. J., Westlake, J. H., Sibeck, D. G., Turner, D. L., Fennell, J. F., Blake, J. B., Jaynes, A. N., Leonard, 580 T. W., Baker, D. N., Spence, H. E., Reeves, G. D., Giles, B. J., Strangeway, R. J., Torbert, R. B., and Burch, J. L.: Statistical analysis of MMS observations of energetic electron escape observed at/beyond the dayside magnetopause, *Journal of Geophysical Research (Space Physics)*, 122, 9440–9463, <https://doi.org/10.1002/2017JA024401>, 2017.
- Daldorff, L. K. S., Tóth, G., Gombosi, T. I., Lapenta, G., Amaya, J., Markidis, S., and Brackbill, J. U.: Two-way coupling of a global Hall magnetohydrodynamics model with a local implicit particle-in-cell model, *Journal of Computational Physics*, 268, 236–254, 585 <https://doi.org/10.1016/j.jcp.2014.03.009>, 2014.
- Dimmock, A. P. and Nykyri, K.: The statistical mapping of magnetosheath plasma properties based on THEMIS measurements in the magnetosheath interplanetary medium reference frame, *Journal of Geophysical Research (Space Physics)*, 118, 4963–4976, <https://doi.org/10.1002/jgra.50465>, 2013.
- Dimmock, A. P., Nykyri, K., and Pulkkinen, T. I.: A statistical study of magnetic field fluctuations in the dayside magnetosheath 590 and their dependence on upstream solar wind conditions, *Journal of Geophysical Research (Space Physics)*, 119, 6231–6248, <https://doi.org/10.1002/2014JA020009>, 2014.
- Dimmock, A. P., Nykyri, K., Karimabadi, H., Osmane, A., and Pulkkinen, T. I.: A statistical study into the spatial distribution and dawn-dusk asymmetry of dayside magnetosheath ion temperatures as a function of upstream solar wind conditions, *Journal of Geophysical Research (Space Physics)*, 120, 2767–2782, <https://doi.org/10.1002/2014JA020734>, 2015a.

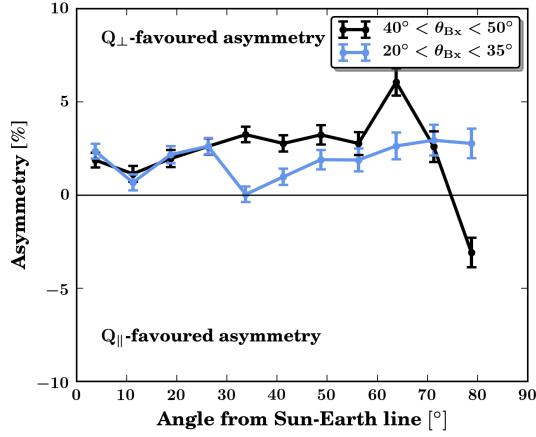
- 595 Dimmock, A. P., Osmane, A., Pulkkinen, T. I., and Nykyri, K.: A statistical study of the dawn-dusk asymmetry of ion temperature anisotropy and mirror mode occurrence in the terrestrial dayside magnetosheath using THEMIS data, *Journal of Geophysical Research (Space Physics)*, 120, 5489–5503, <https://doi.org/10.1002/2015JA021192>, 2015b.
- Dimmock, A. P., Nykyri, K., Osmane, A., and Pulkkinen, T. I.: Statistical mapping of ULF Pc3 velocity fluctuations in the Earth's dayside magnetosheath as a function of solar wind conditions, *Advances in Space Research*, 58, 196–207, <https://doi.org/10.1016/j.asr.2015.09.039>, 2016a.
- Dimmock, A. P., Pulkkinen, T. I., Osmane, A., and Nykyri, K.: The dawn-dusk asymmetry of ion density in the dayside magnetosheath and its annual variability measured by THEMIS, *Annales Geophysicae*, 34, 511–528, <https://doi.org/10.5194/angeo-34-511-2016>, 2016b.
- Dimmock, A. P., Nykyri, K., Osmane, A., Karimabadi, H., and Pulkkinen, T. I.: Dawn-Dusk Asymmetries of the Earth's Dayside Magnetosheath in the Magnetosheath Interplanetary Medium Reference Frame, chap. 5, pp. 49–72, American Geophysical Union (AGU), <https://doi.org/10.1002/9781119216346.ch5>, <https://agupubs.onlinelibrary.wiley.com/doi/abs/10.1002/9781119216346.ch5>, 2017.
- 605 Dubart, M., Ganse, U., Osmane, A., Johlander, A., Battarbee, M., Grandin, M., Pfau-Kempf, Y., Turc, L., and Palmroth, M.: Resolution dependence of magnetosheath waves in global hybrid-Vlasov simulations, *Annales Geophysicae Discussions*, 2020, 1–23, <https://doi.org/10.5194/angeo-2020-24>, <https://angeo.copernicus.org/preprints/angeo-2020-24/>, 2020.
- Eastwood, J. P., Nakamura, R., Turc, L., Mejnertsen, L., and Hesse, M.: The Scientific Foundations of Forecasting Magnetospheric Space Weather, *Space Science Reviews*, 212, 1221–1252, <https://doi.org/10.1007/s11214-017-0399-8>, 2017.
- Formisano, V., Hedgecock, P. C., Moreno, G., Palmiotto, F., and Chao, J. K.: Solar wind interaction with the Earth's magnetic field: 2. Magnetohydrodynamic bow shock, *Journal of Geophysical Research*, 78, 3731, <https://doi.org/10.1029/JA078i019p03731>, 1973.
- Génot, V., Budnik, E., Hellinger, P., Passot, T., Belmont, G., Trávníček, P. M., Sulem, P. L., Lucek, E., and Dandouras, I.: Mirror structures above and below the linear instability threshold: Cluster observations, fluid model and hybrid simulations, *Annales Geophysicae*, 27, [601–615](https://doi.org/10.5194/angeo-27-601-2009), <https://doi.org/10.5194/angeo-27-601-2009>, 2009.
- 615 Hannuksela, O. and the Vlasiator team: Analysator: python analysis toolkit, Github repository, <https://github.com/fmihpc/analysator/>, last access: 09.03.2020, 2020.
- Henry, Z. W., Nykyri, K., Moore, T. W., Dimmock, A. P., and Ma, X.: On the Dawn-Dusk Asymmetry of the Kelvin-Helmholtz Instability Between 2007 and 2013, *Journal of Geophysical Research (Space Physics)*, 122, 11,888–11,900, <https://doi.org/10.1002/2017JA024548>, 2017.
- 620 Herčík, D., Trávníček, P. M., Johnson, J. R., Kim, E.-H., and Hellinger, P.: Mirror mode structures in the asymmetric Hermean magnetosheath: Hybrid simulations, *Journal of Geophysical Research (Space Physics)*, 118, 405–417, <https://doi.org/10.1029/2012JA018083>, 2013.
- Hoilijoki, S., Palmroth, M., Walsh, B. M., Pfau-Kempf, Y., von Althaus, S., Ganse, U., Hannuksela, O., and Vainio, R.: Mirror modes in the Earth's magnetosheath: Results from a global hybrid-Vlasov simulation, *Journal of Geophysical Research (Space Physics)*, 121, [4191–4204](https://doi.org/10.1002/2015JA022026), <https://doi.org/10.1002/2015JA022026>, 2016.
- 625 Hoilijoki, S., Ganse, U., Sibeck, D. G., Cassak, P. A., Turc, L., Battarbee, M., Fear, R. C., Blanco-Cano, X., Dimmock, A. P., Kilpua, E. K. J., Jarvinen, R., Juusola, L., Pfau-Kempf, Y., and Palmroth, M.: Properties of Magnetic Reconnection and FTEs on the Dayside Magnetopause With and Without Positive IMF B_x Component During Southward IMF, *Journal of Geophysical Research (Space Physics)*, 124, 4037–4048, <https://doi.org/10.1029/2019JA026821>, 2019.
- 630 Karimabadi, H., Roytershteyn, V., Vu, H. X., Omelchenko, Y. A., Scudder, J., Daughton, W., Dimmock, A., Nykyri, K., Wan, M., Sibeck, D., Tatineni, M., Majumdar, A., Loring, B., and Geveci, B.: The link between shocks, turbulence, and magnetic reconnection in collisionless plasmas, *Physics of Plasmas*, 21, 062308, <https://doi.org/10.1063/1.4882875>, 2014.

- King, J. H. and Papitashvili, N. E.: Solar wind spatial scales in and comparisons of hourly Wind and ACE plasma and magnetic field data, *Journal of Geophysical Research (Space Physics)*, 110, A02104, <https://doi.org/10.1029/2004JA010649>, 2005.
- 635 Lavraud, B. and Borovsky, J. E.: Altered solar wind-magnetosphere interaction at low Mach numbers: Coronal mass ejections, *Journal of Geophysical Research (Space Physics)*, 113, A00B08, <https://doi.org/10.1029/2008JA013192>, 2008.
- Lavraud, B., Larroque, E., Budnik, E., Génot, V., Borovsky, J. E., Dunlop, M. W., Foullon, C., Hasegawa, H., Jacquy, C., Nykyri, K., Ruffenach, A., Taylor, M. G. G. T., Dandouras, I., and Rème, H.: Asymmetry of magnetosheath flows and magnetopause shape during low Alfvén Mach number solar wind, *Journal of Geophysical Research (Space Physics)*, 118, 1089–1100, <https://doi.org/10.1002/jgra.50145>,
640 2013.
- Lin, Y. and Wang, X. Y.: Three-dimensional global hybrid simulation of dayside dynamics associated with the quasi-parallel bow shock, *Journal of Geophysical Research (Space Physics)*, 110, A12216, <https://doi.org/10.1029/2005JA011243>, 2005.
- Longmore, M., Schwartz, S. J., Geach, J., Cooling, B. M. A., Dandouras, I., Lucek, E. A., and Fazakerley, A. N.: Dawn-dusk asymmetries and sub-Alfvénic flow in the high and low latitude magnetosheath, *Annales Geophysicae*, 23, 3351–3364, <https://doi.org/10.5194/angeo-23-3351-2005>, 2005.
- 645 Lucek, E. A., Constantinescu, D., Goldstein, M. L., Pickett, J., Pinçon, J. L., Sahraoui, F., Treumann, R. A., and Walker, S. N.: The Magnetosheath, *Space Science Reviews*, 118, 95–152, <https://doi.org/10.1007/s11214-005-3825-2>, 2005.
- Modolo, R., Hess, S., Génot, V., Leclercq, L., Leblanc, F., Chaufray, J. Y., Weill, P., Gangloff, M., Fedorov, A., Budnik, E., Bouchemit, M., Steckiewicz, M., André, N., Beigbeder, L., Popescu, D., Toniutti, J. P., Al-Ubaidi, T., Khodachenko, M., Brain, D., Curry, S., Jakosky, B., and Holmström, M.: The LatHyS database for planetary plasma environment investigations: Overview and a case study of data/model
650 comparisons, *Planetary and Space Science*, 150, 13–21, <https://doi.org/10.1016/j.pss.2017.02.015>, 2018.
- Němeček, Z., Šafránková, J., Zastenker, G. N., Pišoft, P., and Paularena, K. I.: Spatial distribution of the magnetosheath ion flux, *Advances in Space Research*, 30, 2751–2756, [https://doi.org/10.1016/S0273-1177\(02\)80402-1](https://doi.org/10.1016/S0273-1177(02)80402-1), 2002.
- Němeček, Z., M., H., Šafránková, J., Zastenker, G. N., and Richardson, J. D.: The dawn-dusk asymmetry of the magnetosheath: INTERBALL-1 observations, *Advances in Space Research*, 31, 1333 – 1340, [https://doi.org/https://doi.org/10.1016/S0273-1177\(03\)00007-3](https://doi.org/https://doi.org/10.1016/S0273-1177(03)00007-3), 2003.
- 655 Nykyri, K., Ma, X., Dimmock, A., Foullon, C., Otto, A., and Osmane, A.: Influence of velocity fluctuations on the Kelvin-Helmholtz instability and its associated mass transport, *Journal of Geophysical Research (Space Physics)*, 122, 9489–9512, <https://doi.org/10.1002/2017JA024374>, 2017.
- 660 Omidi, N., Blanco-Cano, X., and Russell, C. T.: Macrostructure of collisionless bow shocks: 1. Scale lengths, *Journal of Geophysical Research (Space Physics)*, 110, A12212, <https://doi.org/10.1029/2005JA011169>, 2005.
- Omidi, N., Sibeck, D., Gutynska, O., and Trattner, K. J.: Magnetosheath filamentary structures formed by ion acceleration at the quasi-parallel bow shock, *Journal of Geophysical Research: Space Physics*, 119, 2593–2604, <https://doi.org/10.1002/2013JA019587>, <http://dx.doi.org/10.1002/2013JA019587>, 2014.
- 665 Palmroth, M.: Vlasiator, Web site, <https://www.helsinki.fi/en/researchgroups/vlasiator/>, last access: 09.03.2020, 2020.
- Palmroth, M. and the Vlasiator team: Vlasiator: hybrid-Vlasov simulation code, Github repository, <https://github.com/fmihpc/vlasiator/>, version 5.0, last access: 09.03.2020, 2020.
- Palmroth, M., Ganse, U., Pfau-Kempf, Y., Battarbee, M., Turc, L., Brito, T., Grandin, M., Hoilijoki, S., Sandroos, A., and von Althaus, S.: Vlasov methods in space physics and astrophysics, *Living Reviews in Computational Astrophysics*, 4, 1, <https://doi.org/10.1007/s41115-018-0003-2>, 2018.
- 670

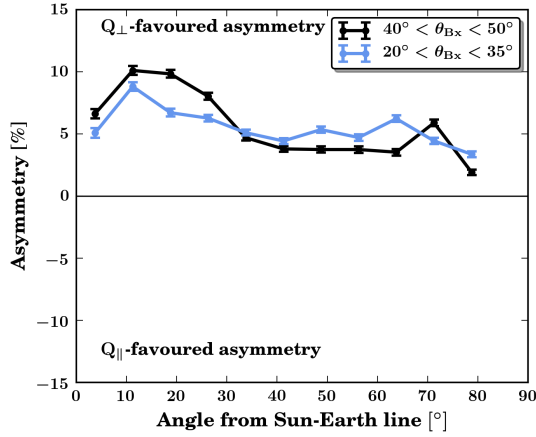
- Paularena, K. I., Richardson, J. D., Kolpak, M. A., Jackson, C. R., and Siscoe, G. L.: A dawn-dusk density asymmetry in Earth's magnetosheath, *Journal of Geophysical Research*, 106, 25 377–25 394, <https://doi.org/10.1029/2000JA000177>, 2001.
- Petrinec, S. M., Mukai, T., Nishida, A., Yamamoto, T., Nakamura, T. K., and Kokubun, S.: Geotail observations of magnetosheath flow near the magnetopause, using Wind as a solar wind monitor, *Journal of Geophysical Research*, 102, 26 943–26 960, <https://doi.org/10.1029/97JA01637>, 1997.
- 675 Pfau-Kempf, Y., Hietala, H., Milan, S. E., Juusola, L., Hoilijoki, S., Ganse, U., von Althaus, S., and Palmroth, M.: Evidence for transient, local ion foreshocks caused by dayside magnetopause reconnection, *Annales Geophysicae*, 34, 943–959, <https://doi.org/10.5194/angeo-34-943-2016>, 2016.
- Pfau-Kempf, Y., Battarbee, M., Ganse, U., Hoilijoki, S., Turc, L., von Althaus, S., Vainio, R., and Palmroth, M.: On the importance of spatial and velocity resolution in the hybrid-Vlasov modeling of collisionless shocks, *Frontiers in Physics - Plasma Physics*, 6, <https://doi.org/10.3389/fphy.2018.00044>, 2018.
- 680 Pulkkinen, T. I., Dimmock, A. P., Lakka, A., Osmane, A., Kilpua, E., Myllys, M., Tanskanen, E. I., and Viljanen, A.: Magnetosheath control of solar wind-magnetosphere coupling efficiency, *Journal of Geophysical Research (Space Physics)*, 121, 8728–8739, <https://doi.org/10.1002/2016JA023011>, 2016.
- 685 Samsonov, A. A., Pudovkin, M. I., Gary, S. P., and Hubert, D.: Anisotropic MHD model of the dayside magnetosheath downstream of the oblique bow shock, *Journal of Geophysical Research*, 106, 21 689–21 700, <https://doi.org/10.1029/2000JA900150>, 2001.
- Sandroos, A.: VLSV: file format and tools, Github repository, <https://github.com/fmihpc/vlsv/>, last access: 09.03.2020, 2019.
- Schwartz, S. J., Burgess, D., and Moses, J. J.: Low-frequency waves in the Earth's magnetosheath: present status, *Annales Geophysicae*, 14, 1134–1150, <https://doi.org/10.1007/s00585-996-1134-z>, 1996.
- 690 Shue, J. H., Chao, J. K., Fu, H. C., Russell, C. T., Song, P., Khurana, K. K., and Singer, H. J.: A new functional form to study the solar wind control of the magnetopause size and shape, *Journal of Geophysical Research (Space Physics)*, 102, 9497–9512, <https://doi.org/10.1029/97JA00196>, 1997.
- Soucek, J., Lucek, E., and Dandouras, I.: Properties of magnetosheath mirror modes observed by Cluster and their response to changes in plasma parameters, *Journal of Geophysical Research (Space Physics)*, 113, A04203, <https://doi.org/10.1029/2007JA012649>, 2008.
- 695 Soucek, J., Escoubet, C. P., and Grison, B.: Magnetosheath plasma stability and ULF wave occurrence as a function of location in the magnetosheath and upstream bow shock parameters, *Journal of Geophysical Research (Space Physics)*, 120, 2838–2850, <https://doi.org/10.1002/2015JA021087>, 2015.
- Spreiter, J. R., Summers, A. L., and Alksne, A. Y.: Hydromagnetic flow around the magnetosphere, *Planetary and Space Science*, 14, [https://doi.org/10.1016/0032-0633\(66\)90124-3](https://doi.org/10.1016/0032-0633(66)90124-3), 1966.
- 700 Tótrallyay, M. and Erdős, G.: Statistical investigation of mirror type magnetic field depressions observed by ISEE-1, *Planet. Space Sci.*, 53, 33–40, <https://doi.org/10.1016/j.pss.2004.09.026>, 2005.
- Trávníček, P., Hellinger, P., Taylor, M. G. G. T., Escoubet, C. P., Dandouras, I., and Lucek, E.: Magnetosheath plasma expansion: Hybrid simulations, *Geophysical Research Letters*, 34, L15104, <https://doi.org/10.1029/2007GL029728>, 2007.
- Treumann, R. A.: Fundamentals of collisionless shocks for astrophysical application, 1. Non-relativistic shocks, *Astronomy and Astrophysics Review*, 17, 409–535, <https://doi.org/10.1007/s00159-009-0024-2>, 2009.
- 705 Turc, L., Fontaine, D., Savoini, P., and Kilpua, E. K. J.: A model of the magnetosheath magnetic field during magnetic clouds, *Ann. Geophys.*, 32, 157–173, <https://doi.org/10.5194/angeo-32-157-2014>, 2014.

- Turc, L., Fontaine, D., Savoini, P., and Modolo, R.: 3D hybrid simulations of the interaction of a magnetic cloud with a bow shock, *Journal of Geophysical Research (Space Physics)*, 120, 6133–6151, <https://doi.org/10.1002/2015JA021318>, 2015.
- 710 Turc, L., Escoubet, C. P., Fontaine, D., Kilpua, E. K. J., and Enestam, S.: Cone angle control of the interaction of magnetic clouds with the Earth's bow shock, *Geophysical Research Letters*, 43, 4781–4789, <https://doi.org/10.1002/2016GL068818>, 2016.
- Turc, L., Ganse, U., Pfau-Kempf, Y., Hoilijoki, S., Battarbee, M., Juusola, L., Jarvinen, R., Brito, T., Grandin, M., and Palmroth, M.: Foreshock Properties at Typical and Enhanced Interplanetary Magnetic Field Strengths: Results From Hybrid-Vlasov Simulations, *Journal of Geophysical Research (Space Physics)*, 123, 5476–5493, <https://doi.org/10.1029/2018JA025466>, 2018.
- 715 von Alfthan, S., Pokhotelov, D., Kempf, Y., Hoilijoki, S., Honkonen, I., Sandroos, A., and Palmroth, M.: Vlasiator: First global hybrid-Vlasov simulations of Earth's foreshock and magnetosheath, *Journal of Atmospheric and Solar-Terrestrial Physics*, 120, 24–35, <https://doi.org/10.1016/j.jastp.2014.08.012>, 2014.
- Walsh, A. P., Haaland, S., Forsyth, C., Keesee, A. M., Kissinger, J., Li, K., Runov, A., Soucek, J., Walsh, B. M., Wing, S., and Taylor, M. G. G. T.: Dawn-dusk asymmetries in the coupled solar wind-magnetosphere-ionosphere system: a review, *Annales Geophysicae*, 32, 705–737, <https://doi.org/10.5194/angeo-32-705-2014>, 2014.
- 720 Walsh, B. M., Sibeck, D. G., Wang, Y., and Fairfield, D. H.: Dawn-dusk asymmetries in the Earth's magnetosheath, *Journal of Geophysical Research (Space Physics)*, 117, A12211, <https://doi.org/10.1029/2012JA018240>, 2012.
- Walters, G. K.: Effect of Oblique Interplanetary Magnetic Field on Shape and Behavior of the Magnetosphere, *Journal of Geophysical Research*, 69, 1769–1783, <https://doi.org/10.1029/JZ069i009p01769>, 1964.
- 725 Wang, Y., Raeder, J., and Russell, C.: Plasma depletion layer: Magnetosheath flow structure and forces, *Annales Geophysicae*, 22, 1001–1017, <https://doi.org/10.5194/angeo-22-1001-2004>, 2004.
- Wing, S., Johnson, J. R., Newell, P. T., and Meng, C. I.: Dawn-dusk asymmetries, ion spectra, and sources in the northward interplanetary magnetic field plasma sheet, *Journal of Geophysical Research (Space Physics)*, 110, A08205, <https://doi.org/10.1029/2005JA011086>, 2005.
- 730 Winterhalter, D. and Kivelson, M. G.: Observations of the Earth's bow shock under high Mach number/high plasma beta solar wind conditions, *Geophysical Research Letters*, 15, 1161–1164, <https://doi.org/10.1029/GL015i010p01161>, 1988.
- Zwan, B. J. and Wolf, R. A.: Depletion of solar wind plasma near a planetary boundary, *Journal of Geophysical Research*, 81, 1636, <https://doi.org/10.1029/JA081i010p01636>, 1976.

Magnetic field strength (central magnetosheath)



Bulk velocity (central magnetosheath)



Ion density (central magnetosheath)

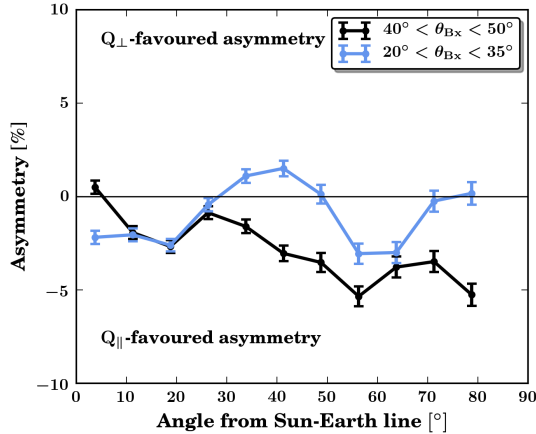


Figure 7. Asymmetries in the central magnetosheath as obtained from statistics of THEMIS spacecraft observations. From top to bottom: magnetic field strength, bulk velocity and ion density. The black curves correspond to data with a cone angle near the Parker spiral orientation ($40^\circ < \theta_{Bx} < 50^\circ$) and the blue curves to data with a low cone angle values ($20^\circ < \theta_{Bx} < 35^\circ$).